LASER INDUCED GAS BREAKDOWN IN THE PRESENCE OF STATIC ELECTRIC FIELD AND METAL SURFACE

by

VINAY KUMAR

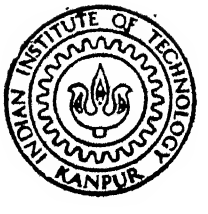

DEPARTMENT OF PHYSICS

INDIAN INSTITUTE OF TECHNOLOGY KANPUR

SEPTEMBER, 1989

LASER INDUCED GAS BREAKDOWN IN THE PRESENCE OF STATIC ELECTRIC FIELD AND METAL SURFACE

A Thesis Submitted
in Partial Fulfilment of the Requirements
for the Degree of

DOCTOR OF PHILOSOPHY

by

VINAY KUMAR

to the

DEPARTMENT OF PHYSICS
NDIAN INSTITUTE OF TECHNOLOGY KANPUR

SEPTEMBER, 1989

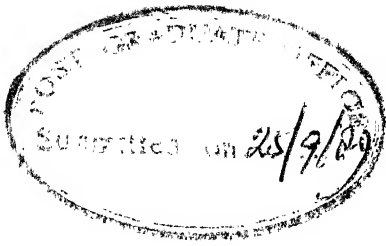

CERTIFICATE

Certified that the work contained in the thesis entitled **"Laser Induced Gas Breakdown in the Presence of Static Electric Field and Metal Surface"** has been carried out by Mr. Vinay Kumar under my supervision and the same has not been submitted elsewhere for a degree.

RK Thareja

Kanpur
September 25, 1989

(Dr R K THAREJA)
Thesis Supervisor

ACKNOWLEDGEMENTS

I am deeply indebted to Dr. R.K.Thareja for introducing me to the subject and for supervising my work with keen interest. Working with him has been a rich experience and I shall always cherish it. It was very enjoyable being introduced by him to the methodology of research.

I am thankful to my lab mates Alika, Dharmaraj, Neena, Rekha and Sridevi for their cooperation.

Technical assistance by the staff of the CELT and the Glass blowing workshops is highly acknowledged.

I would like to thank Messrs Jagir Singh, A.C.Joshi and Joseph John of ACES for their prompt help as and when required.

Thanks are due to Mr. A.K. Srivastava for typing the manuscript and Mr. R.K. Bajpai for preparing the tracings.

I would also like to thank my friends Alok, Anuradha, Alika, Dada, Godre, KK, Manu, Raghava, Raje, Ravi, Rekha, Srini, Subba Rao and Sivasubramanium who have made my stay memorable at I.I.T. Kanpur.

Finally, I thank my parents for encouraging me in my pursuits, for standing by me when things didn't seem to go well and more importantly for allowing me to chase my own dreams. They made me what I am today and it is to them that I owe everything I have.

Vinay Kumar

LIST OF PUBLICATIONS

1. A Khare, V Kumar, and R K Thareja (1987), *'On Studies of Spontaneously Emitted* Cd I *and* Cd II *Lasing Transitions'*, Z. Phys. D-Atoms Mol and Clusters 6, 67.

2. V Kumar and R K Thareja (1988), *'Laser Produced Plasma Using an Excimer Laser'*, Bull. Am. Phys. Soc. 33, 1653.

3. V Kumar and R K Thareja (1988), *'Laser Induced Gas Breakdown in the Presence of a Static Electric Field'*, J. Appl. Phys. 64, 5269.

4. V Kumar and R K Thareja, *'Studies of Excimer Laser Produced Copper Plasma in the Presence of Background Gas'*, J. Appl. Phys. to appear.

5. V Kumar and R K Thareja , *'Laser Induced Breakdown of Argon Gas Near Metal Surface'*, Appl. Phys. B (submitted).

6. V Kumar and R K Thareja , *'Laser Induced Gas Breakdown: A Plasma Switch'*, Phys. Lett. A (submitted).

7. V Kumar, A C Joshi, and R K Thareja, *'Low Cost Microprocessor Controlled Scan System for Monochromator'* Eur. J. Phys. (submitted).

TABLE OF CONTENTS

LIST OF FIGURES

LIST OF TABLES

LIST OF SYMBOLS

Γ_r Width of the intermediate level.

Δt Delay between rise time for the peak laser intensity and maximum surface temperature.

ε_o Permittivity of free space.

λ Wavelength.

λ_D Debye length.

$\bar{\nu}$ Wave number of the electron.

ν_c Collision frequency.

σ_{ea} Elastic scattering cross section.

τ_E Width of photocurrent pulse.

τ_L Width of laser pulse.

Ω Volume of emitting surface.

A Atomic weight.

A_i Constant, depends on the gas.

A_p Transition probability.

$A_{th} = \frac{4\pi\ m\ K^2 e}{h^3} = 120\ \text{Amp/cm}^2\ \text{deg}^2$.

a Laser pulse parameter.

b Laser pulse parameter.

C Velocity of light.

D Thermal diffusivity.

d Distance between electrodes.

E Excitation energy of the level.

E_ϕ Work function of the metal.

E_F Fermi Energy.

E_i Ionization energy of the atom.

E_o Energy of the ground state.

E_p Photon energy.

E_r Energy of the near resonance intermediate level.

e Electronic charge.

g Statistical weight of level.

h Planck constant.

I Incident laser intensity.

I_o Peak laser intensity.

i Photo current.

i_o Peak photo current.

j Current density.

j_{th} Thermionic current density.

K Boltzmann's constant.

K_c Thermal Conductivity.

k Number of photons required to ionize the gas.

$K_{f,g}^{(k)}$ k^{th} order matrix element for the transition between initial bound state $|g\rangle$ and final state $|f\rangle$.

k_o Number of photons actually involved in ionizing the gas.

M_B Mass of background gas atom.

m Electron mass.

N Number of excited electrons per second.

n Number of photons involved in electron emission from target surface.

n_B Background gas atom density.

n_e Electron density.

p Pressure of the gas.

$Q_{\Delta T}$ Loss of energy in elastic collision between electron and buffer gas atom.

R Surface reflectivity.

r Current measuring resistance.

r_o Classical electron radius.

s Radiation spot size.

T_e Electron temperatures.

T_s Surface temperature.

t Time to develope cascade.

u Speed of sound in vapor.

W Ionization probability.

x Defocussing parameter.

x_p Distance from metal surface.

Z Charge on ion.

z Surface depth.

SYNOPSIS

LASER INDUCED GAS BREAKDOWN IN THE PRESENCE OF STATIC ELECTRIC FIELD AND METAL SURFACE

Submitted in partial fulfilment of the requirements
for the degree of

DOCTOR OF PHILOSOPHY

by

VINAY KUMAR

to the

DEPARTMENT OF PHYSICS
INDIAN INSTITUTE OF TECHNOLOGY
KANPUR 208 016 INDIA

In this thesis we report the studies on Excimer laser induced breakdown of rare gases, in presence of static electric field and near metal surface. Some studies on laser produced metal plasma are also reported. An attempt is made to utilize the effect of metal plasma on laser induced breakdown of argon gas in various configurations of biased target, to explore the possibility of a plasma switch.

Laser induced gas breakdown studies were performed by focusing a low power excimer laser (XeCl 308 nm) radiation in a specially designed discharge cell. The discharge cell contains two parallel plate electrodes separated by a distance of 6.5 mm. Both ends of the electrodes were tapered to 2 mm width and

taken out from the glass cell through the holes, to apply the static voltage. This Transverse Static Electric Field (TSEF) was used to partially excite the gas atoms. A metal target was inserted later in the discharge cell to provide preionization/ initial electrons. Ionization current of the order of 10^{-8} Amp measured in terms of voltage drop across a resistance connected in series with one of the electrodes was considered to be the breakdown current. The voltage pulse was displayed on the storage oscilloscope. Studies on breakdown of Neon, Argon and Xenon gases were performed. Metal plasma was produced by focusing the excimer laser radiation on to the copper target in the presence of background gas. A Microprocessor Controlled Scan System (MCSS) was developed for monochromator to scan the visible spectrum of radiation emitted from metal plasma. The output from the monochromator was detected with a photomultiplier tube (PMT). The PMT output signal was displayed on the storage oscilloscope and recorded on the chart recorder.

Breakdown of Ne, Ar and Xe gases at various pressures, in the range of 0.2 - 24.0 torr, is studied by focusing a low power excimer laser in the presence of static electric field transverse to the laser focus. Results are similar to that observed with high power laser. Ionization is proposed to be a two step process, initial excitation being through collision of atoms with electrons due to TSEF followed by photoionization in

the presence of laser. We report for the first time that k_o, the number of photons actually involved to ionize the gas in the experiment, decreases with the increase of static electric field.

Laser induced breakdown of Argon gas near metal surface is studied by using low power excimer laser in the presence of TSEF. We report for the first time that photoelectric emission from metal surface dominates over the thermionic emission and reduces the threshold laser energy required to breakdown Argon gas. Ionization current is observed to be dependent on laser induced photo-electric emission from target surface.

Spatial and temporal behavior of the emission spectrum of excimer laser produced copper plasma, in vacuum and in the presence of background gas, are studied. It is observed that spontaneous emission from Cu I lasing transition $4p\ ^2P_{3/2} - 4s^2\ ^2D_{5/2}$ at 510.5 nm shows a strong dependence on pressure of neon gas. We report the possibility of getting copper vapor lasing transition $4p\ ^2P_{3/2} - 4s^2\ ^2D_{5/2}$ at 510.5 nm as a result of recombination in presence of neon gas. The plasma temperature was estimated, by assuming the plasma to be in Local Thermodynamic Equilibrium (LTE) and by taking the ratio of intensity of two spectral lines. The temperature is estimated to lie in the range 0.6 ev $\leq T_e \leq$ 0.8 ev for Cu I in the presence of argon gas at a pressure of 8 torr. The velocity of propagation

of the plasma emission front at 3 mm away from the target surface is found to be 4.8 x 10^5 cm/sec in argon gas at a pressure of 8 torr and 1.5 x 10^6 cm/sec in vacuum. It is also observed that intensity of many emitted spectral lines increases in the presence of background gas. The presence of surrounding gas can thus improves the accuracy of laser microspectral analysis.

The effect of metal plasma, formed on the surface of a biased target, on laser induced breakdown of argon gas is studied in various configurations of biased target. It is observed that the effect of metal plasma in our studies is identical to the function of grid between anode and cathode in a triode. We report for the first time that ionization of argon gas can be switched ON or OFF either keeping laser focusing conditions fixed and by changing the polarity OR keeping the polarity fixed and by changing the laser irradiation.

CHAPTER 1

INTRODUCTION

The interaction of light with matter has been the subject of many theoretical and experimental investigations for more than two decades. Since the first report [1,2] on gas breakdown at optical frequencies by means of a Q-switched laser, there have been many reports on optical breakdown of gaseous medium [3-5] as well as condensed matter [6,7]. The phenomenon is observable at very high field strengths (> 10^6 V/cm for atmospheric gases [4]), the fields which can easily be obtained by focusing a high power laser beam. Laser field as strong as coulomb field applied to an atom rips the valence electron away from an atom and the gas breakdown is observed. Breakdown of gaseous medium is defined by a visual flash or spark, just as in ordinary gas discharge, whereas it is the appearance of a damage spot in solids and of a cavity in liquids. Laser induced gaseous and metal plasmas have several applications in various fields of research. Laser triggered spark gaps [8] have been developed and extensively used in high voltage switches. The possibility of generating thermonuclear reactions was suggested by Nuckolls et al [9], since then a significant achievements have been made in this field. Several sensitive techniques to measure UV radiation based on photoionization of excited atoms have been developed [10]. Laser induced rare gas plasmas are

found as a source of VUV radiations [11]. Laser oscillations have been observed in laser produced recombining plasmas in IR [12,13] to XUV [14]. Extensive studies are being performed for exploring the possibility of short wavelength lasers [15] by irradiating carbon fibre target with laser beams of high intensity. Laser produced metal plasmas have been used as a source of high intensity X - rays [16], and for photoionization lasers [17]. Recently plasma induced by low power lasers has been used for laser microspectral analysis [18,19].

Solids and gaseous medium exhibit different breakdown characteristics, I will discuss the laser induced breakdown of gases and solids separately.

Laser induced gas breakdown

There are two main mechanisms by which a gas (atom) can be ionized in the field of an intense electromagnetic wave: direct multiphoton ionization (MPI) and electron impact or cascade ionization.

Multiphoton ionization This process takes place with laser beam of intensity $\geq 10^{11} W/cm^2$, involves ionization of isolated atom or molecule, ionization of one atom does not affect that of the other. In other words the gas pressure must be low, $\leq 10^{-3}$ torr. At such low pressures the mean free path of electrons created by multiphoton ionization is much larger than the dimension of the focal volume in which ionization occurs.

Also, the time interval separating two successive collisions (10^{-6} sec) is much greater than the duration of the laser pulse (10^{-8} sec). Thus, under such conditions no collision takes place among charged particles or neutrals and hence the ionization is free of secondary effects like cascade or avalanche ionization. The process is self sufficient in the sense, an atom or molecule of ionization energy E_i absorbs k photons of energy $h\nu$ simultaneously subject to the condition $kh\nu \geq E_i$ and thereby becomes photoionized, where $k = \langle \frac{E_i}{E_p} \rangle$, E_i and E_p being the ionization energy of the atom and photon energy respectively, the angle bracket indicates next larger integer of the quantity. In general the ionization probability W of an atom absorbing simultaneously k photons is given by

$$W = A_i I^k \qquad (1).$$

where I is the intensity of laser beam and A_i is a constant which depends on the particular gas under investigation. Several authors [20-25] have evaluated the ionization probability W using k^{th} order time dependent perturbation theory. Following Bebb and Gold [21], the coefficient A_i is given by

$$A_i = \frac{m}{2\pi h} \left[\frac{4\pi^2 e^2}{h C}\right]^k | K_{f,g}^{(k)}|^2 \bar{\nu} \qquad (2).$$

where $K_{f,g}^{(k)}$ represents the k^{th} - order matrix element for the transition between initial bound state $|g\rangle$ and final $|f\rangle$ state

in the continuum, e and m are the charge and mass of the electron respectively and $\bar{\nu}$ its wave number. The analysis takes account of the presence of intermediate energy states. The main contribution due to intermediate states comes only if intermediate state energy and the energy of an integral number of quanta are very close. They concluded that although MPI may provide the initial electron, it does not account entirely for the breakdown phenomenon, except possibly at very low pressure. It was also shown that threshold flux for MPI varies with pressure as $p^{-1/k}$, a very weak pressure dependence on threshold flux, and hence the presence of any low ionization trace impurities in the gas will enhance [26] the probability of providing initiating electron. The main difficulty in the evaluation of A_i and W lies in the choice of appropriate wavefunction. It has been shown [23,27,28] that the large laser field intensity can induce level broadening and the displacement of the intermediate states. They showed that multiphoton ionization rate is proportional to I^k multiplied by the sum of terms of the form $\left\{ [E_r - E_o - (k-1)h\nu]^2 + \Gamma_r^2 \right\}^{-1}$ in which E_r is the energy of a near-resonance intermediate level, E_o is the ground state energy and Γ_r is the width of the intermediate level.

Using a semi-classical approach, Keldysh [29] derived the generalized formula for the probability of ionization by a

strong electric field associated with strong radiation field. In the high frequency limit Keldysh formula for the liberation of electrons describes the multiphoton effect and in the limit of low frequency fields it reduces to tunnel effect. The evaluation of probability of a transition from a bound state to the virtual levels of the continuum spectrum (no quasi-resonant transition) gives results similar to quantum mechanical treatment [21], however, the frequency dependence is somewhat different.

In the case of a perfectly monochromatic beam from a single mode laser there is no fluctuation in intensity, and the value of ionization probability W is given by eqn (1). However, for radiation from a multimode laser there will be large intensity fluctuations and the instantaneous intensity I and the time average intensity $\langle I \rangle$ differs. The intensity dependence in eqn (1) is modified to $I^k = k! \langle I \rangle^k$, the multiphoton ionization probability is increased k! -fold and the threshold intensities are reduced [21,30,31] by a factor $(\frac{1}{k!})^{1/k} \sim \frac{1}{k} \simeq \frac{2}{k}$ compared with thresholds obtained with a single-mode laser having the same average intensity $\langle I \rangle$.

There have been several experimental studies carried out on understanding of MPI process, important ones being [3,4,32-36]. The experiments consist essentially of measuring the number of ions produced as a function of laser intensity in conditions

where cascade ionization by inverse bremsstrahlung absorption can not occur. As stated earlier, this can be obtained if the experiment is performed at low gas density (or pressure) so that the electron and atom free paths are much larger than focal dimensions, and the collision frequencies are much less than the inverse pulse width. In addition it is made sure that low ionization potential hydrocarbons from the ionization chamber are removed. In order to achieve a sufficient intensity to cause MPI, the laser beam is usually focused using lens system. Agostini et al [3] reported such an experiment using laser intensities of the order of 10^{13} W/cm^2 where they observed MPI of He, Ne, Ar, Kr, and Xe using a focused Q-switched Nd: Glass laser (λ = 1.06 μm) and its second harmonic at 0.53 μm into a cell containing gas at a pressure of 10^{-3} torr. They found that irrespective of the nature of the gas or wavelength of light, all the experimental curves for the variation of total number of ions created as a function of laser intensity in the focusing region show similar trends. For low values of light intensity the ionization increases very rapidly with increasing light intensity. The slope of the curve gives the experimental value of k_o, the number of photons actually involved in ionizing the gas. When the light intensity increases beyond a certain value the ionization proceeds less rapidly and slope of all curves approaches a limiting value of two. They attribute this to

saturation process. Similar discontinuity had also been reported by Chin et al. [37,38] in their multiphoton ionization studies of Mercury, Cesium, Potassium, and Xenon. Okuda et al [39-41] have also reported experimental investigations on the pressure dependence of MPI process in Cesium, Rubidium and Sodium. The experimental results are in reasonable agreement with the theoretical predictions of multiphoton theory. Similar agreement have also been reported by Alcock et al [42] and Dewhurst et al [43] using ps pulses of neodymium glass laser in Ar and N_2 gases. All the experiments show a weak pressure dependence in agreement with the theoretical predictions.

Cascade ionization In this process it is necessary that there should be at least one electron in the focal region (at the time of arrival of laser pulse), electrons gain energy from the laser field through inverse bremsstrahlung collisions with the neutrals. Once the energy of the electrons exceeds E_i they can ionize the gas through a binary collision. At sufficiently high fields cascade ionization or electron avalanche follows resulting in the formation of a plasma. Once the plasma is formed the incident light is absorbed by electrons via free-free transition in the field of ions. This causes intense heating of the electron plasma and a consequent rapid hydrodynamic expansion of the plasma in the form of a shockwave [44]. The

final result is the appearance of a spark in the gas and a visible damage in the case of a condensed matter .

Many breakdown measurements have been carried out using ruby (λ=0.6943 μm) and Nd:Glass (λ=1.06 μm) laser. The breakdown criteria used in the experiments is the visible observation of spark, reduction in the laser energy transmitted through the gas in the focal volume or measurement of ion current. Buscher et al [45] were the first to study the breakdown threshold intensity of rare gases at wavelengths 1.06, 0.69, 0.53 and 0.35 μm. They found that the threshold intensity for each rare gas studied first increases to a peak and then decreases with decreasing wavelength. Alcock et al [46] reported the breakdown of nitrogen, methane, air and rare gases using a ruby laser of pulse width 20 ns and its second harmonic, in agreement with Buscher et al [45]. Krasyuk et al [33,34] studied the breakdown threshold of nitrogen, helium and argon using ps pulses of ruby laser in the pressure range $2 \leq p \leq 10^4$ torr. The results show a weak dependence on the pressure for $p \leq 5x10^3$ torr in He and Ar and for $p \leq 3x10^2$ torr in N_2, characteristic of multiphoton absorption. At higher pressure in He and Ar there is a pronounced p dependence, indicating the occurrence of collisional ionization by inverse bremsstrahlung absorption, however for N_2 the p dependence is less pronounced. Alcock et al [42], Dewhurst et al [43,47], and Ireland et al [48] have shown

a strong p dependence at very high pressures using ps pulses of Nd: Yag laser and its second harmonic. They suggested inverse bremsstrahlung absorption to be responsible for breakdown rather than multiphoton absorption at high pressure. Similar dependence has also been reported [49] using ns pulses of ruby laser. The influence of diffusion losses on the breakdown threshold has been investigated [50,51] by using lenses of different focal lengths. Dependence of breakdown threshold intensity on focal length of lens at different pressure of argon is reported by Mitsuk et al [50]. The smaller the focal length, the smaller the dimension of the focal volume, the greater the rate of diffusion of electrons out of it, and hence higher the threshold intensity. The slope of the threshold field versus focal length (of the lens) curve decreases with increasing focal length. Recently [52] breakdown measurements have been reported in N_2 and Ar using XeF excimer laser with pulse length of 500 ns and third harmonic of Nd: glass laser with pulse length of 0.4 ns. Weyl et al [52] and Weyl and Rosen [53] have developed a theory incorporating the multiphoton ionization rate derived from Krasyuk and Pashinin's data [54] and obtained results in agreement with the experiment. Using visible and UV radiation highly excited states can readily be photoionized over times much shorter than the laser pulse [55]. Several authors [53,56,57] have derived the expression for the growth

rate and threshold intensity for breakdown of gases. Detailed calculations of the air breakdown threshold caused by laser irradiation have been carried out by Kroll and Watson [56]. Gamal et al [57] and Weyl et al [53] have done theoretical calculations of laser induced breakdown thresholds of atomic and molecular gases as a function of pressure of the gas, pulse width of laser using the equation of growth of electron, and including the effects of both MPI and cascade ionization.

There have been reports on the observation of gas breakdown with low power lasers in the presence of preionization. The initiatory electron can be provided by static electric field or by metal surface. Smith [58] have shown that preionization densities $\simeq 10^{11}$ cm^{-3} lowers the threshold. Similar results are reported by Robinson [59] for preionization densities as low as 10^{10} cm^{-3}. There have been experimental observations [58,60,61] on breakdown of gases using simultaneously static electric field and laser field both. The partial excitation of the gas due to the electric field is followed by collisional ionization, photoionization of excited atoms (depending on wavelength of laser, gas type, pressure and static field) by laser field. When a D C discharge is illuminated with low intensity laser field, the laser radiation breaks down the gas slightly further, leading to an increase discharge current [61]. Tulip et al [62] studied the effect of applying an electric field transverse

to the laser focus on laser induced breakdown of air. In their experiment, a chamber containing low pressure gas with arrangement for applying static electric field was kept within the cavity of a CO_2 laser. They observed that depending on the field strength, it was possible to induce gas breakdown with low intensity laser field in the presence of a static electric field. Kopeika et al [61] studied the gas breakdown in the townsend region of discharge [63]. They used a Hamamatsu R702 (argon) gas filled phototube, containing semi cylindrical S-5 photo cathode with wire anode along the cylindrical axis as discharge tube and static field was applied to it to operate in townsend region of discharge, chopped radiation from tungsten lamp along with a monochromator was used as a monochromatic light source. They observed that breakdown characteristics are similar to that observed using high power laser alone. In their further work [64] they used 300 ps Nitrogen laser (337 nm) radiation focused perpendicular to the electrode plane in the gas between the electrodes and showed that effects of bias and incident laser field are complementary. We have reported [65] the breakdown of Ne, Ar and Xe gases at different pressures using a XeCl excimer laser in the presence of a static electric field applied transverse to the laser focus.

Pirri et al [66] were the first to report the laser induced gas breakdown near target surface. Bondarenko et al [67] have

observed the decrease in threshold energy required to breakdown the gas using CO_2 laser radiation, not enough to provide avalanche ionization. They attributed the ionization due to thermal explosion process of the gas near the surface of a target. Vedenov et al [68] have shown theoretically that breakdown of a gas is due to thermal ionization of metal vapor of low ionization potential. Dan'shchikov et al [69] showed using CO_2 laser radiation that the decrease may be due to presence of precursor plasma. Barchukov et al [70] have proposed that an electron cascade can develope to ionize the gas surrounding the target due to metal vapor. The minimum intensity, $I(W/cm^2)$, required for the development of an electron cascade in the gas is given by [70]

$$I > 6 \times 10^{9} E_i/\lambda^2 A \qquad (3).$$

where E_i is the first ionization energy (ev) of the gas, λ is the wavelength (μm) of laser radiation and A the atomic (molecular) weight of the gas particle. They reported that an explosion wave (spherical shock wave) near the target surface develops in a small region of dense vapor if the time [70] $t = \frac{s}{u} << \tau_L$, the laser pulse duration, where s is the radiation spot on the surface of the target and u the speed of sound in the vapor. Short wavelength radiation from laser produced metal plasma has also been used [71-73] for investigation of breakdown of ambient gases. It is observed that the presence of metal

plasma reduces the threshold energy required for breakdown of the gas. The photoionization of He and N_2 has been reported due to UV radiation from a laser produced plasma [72]. The plasma was produced by focusing 1.7 ns, 4-J CO_2 laser radiation on to a copper target. We have observed [74] the laser induced breakdown of argon gas near metal surface using a XeCl excimer laser with intensity less than the threshold intensity defined by eqn (3) in the presence of TSEF.

Laser induced metal plasma

The physical mechanism governing optical breakdown in solids is essentially the same as in the gas [75]. The conduction electrons here play the role of free electrons, and excitation of valence electrons to the conduction band is equivalent [76] to ionization of atoms in a gas. When laser light impinges on a solid target the phenomenon observed depends mainly on the incident energy density, duration, wavelength of the laser light and on the physical properties of the target material. The light is either reflected, absorbed or transmitted. For low irradiation ($\simeq 10^6$ W/cm^2), the absorbed radiation appears as heat which is slowly distributed throughout the material by thermal diffusion. For a conducting material, the incident energy is absorbed within a skin depth. At slightly higher irradiation ($> 10^6$ W/cm^2), depending on the thermal conductivity, thermal diffusivity, reflectivity of the target

material and characteristics (or parameters) of laser pulse, intense local heating of the surface will occur resulting in a rise in surface temperature of the material. If the surface temperature is high enough, thermionic emission [6] from the target surface is expected. The photoelectric emission from the target surface using Nd: glass laser (GW/cm^2, ps) has also been reported [77]. As the irradiation increases, the temperature of the surface increases and a molten pool of depth $(D\tau_L)^{1/2}$ is formed, where D is the thermal diffusivity and τ_L is the duration of the laser pulse. A further increase in the irradiation will cause the surface temperature of the molten pool to reach boiling point resulting in evaporation. This will happen when the energy deposited is approximately equal to the latent heat of sublimation [6] L_S (erg/gm) $\simeq I\tau_L^{1/2} \rho^{-1} D^{-1/2}$, where ρ is the density of the solid target and I is intensity of laser radiation. Once the vapor is formed the laser light will cause further heating by multiphoton ionization and inverse bremsstrahlung resulting in a high temperature plasma. At irradiation of 10^8 W/cm^2 it is possible to produce the plasma [78] directly at the focus on to the target due to direct vaporization from the solid without going through the intermediate steps [18]. At sufficiently high irradiation temperature of few hundreds of eV can be produced. We have reported [79] the studies on both spatial and temporal behavior

of the emission spectrum of laser produced plasma (LPP) formed at the copper target in presence of background gas and in vacuum using XeCl (308 nm) excimer laser.

Present work

In the present work we report the studies on Excimer laser induced breakdown of rare gases, in the presence of static electric field and near metal surface. Some studies on laser produced metal plasma are also reported. Effect of metal plasma on laser induced breakdown of argon gas in various configuration of biased target is used to explore the possibility of a plasma switch.

The details of the experimental techniques used in the present work are described in chapter 2.

Chapter 3 describes the results of present work on the excimer laser induced breakdown studies of Ne, Ar and Xe gases, in the pressure range of 0.2 - 24.0 torr, in the presence of static electric field transverse to the laser focus. An attempt is made to find out the variation of k_o, the number of photons actually involved to ionize the gas in the experiment, with static electric field.

Chapter 4 describes the studies on laser induced breakdown of Argon gas near metal surface. Dependence of threshold laser energy on the argon gas pressure with and without metal surface,

at constant static electric field, is reported. Laser induced thermionic current density and two photon photo-current density from target surface is estimated. The effect of electron emission on threshold laser energy required to breakdown argon gas is investigated. An attempt is made to study the temporal profile of photoelectric current pulse.

Studies on spatial and temporal behavior of the emission spectrum of excimer laser produced copper plasma in vacuum and in the presence of background gas are presented in chapter 5. The effect of background gas on the spontaneously emitted lines is reported. The possibility of getting copper vapor lasing transition $4p\ ^2P_{3/2} - 4s^2\ ^2D_{5/2}$ at 510.5 nm as a result of recombination in the presence of neon gas is investigated. The plasma temperature and the velocity of propagation of the plasma emission front are estimated.

Studies on the effect of metal plasma formed at the surface of a biased target on laser induced breakdown of argon gas are presented in chapter 6. Parameters to control the switching of argon gas discharge are investigated.

Chapter 7 summarizes the results of the present work.

CHAPTER 2

EXPERIMENTAL TECHNIQUES

Various experimental techniques used for observing laser induced gas breakdown have been described in Chapter 1. Laser induced breakdown is usually confirmed by visually observing the bright flash at the focus of laser beam or by using charge collector plates. We report the studies on investigation of laser induced gas breakdown in presence of static electric field and near metal surface by measuring the ionization current. Some studies on laser induced metal plasma in vacuum and in the presence of surrounding gas are also reported. Discharge cell as shown in Figure 1 and Figure 2 was designed to study gas breakdown. Figure 2 has an additional metal surface. Transverse Static Electric Field (TSEF) was applied across the plates as shown in Figure 1. Electrodes used are brass plates of dimension 20x25 mm^2, tapered from both the ends to 2 mm width. Tapered ends were taken out from the cell through the holes drilled in the glass cell to apply static electric field. The electrodes were thoroughly cleaned and inserted in a cleaned pyrex glass cell of length 78 mm, outer diameter 33 mm and wall thickness 2.5 mm. The separation between two electrodes was adjusted to 6.5 mm and holes were sealed with epoxy. The windows were also pasted with epoxy. To study the

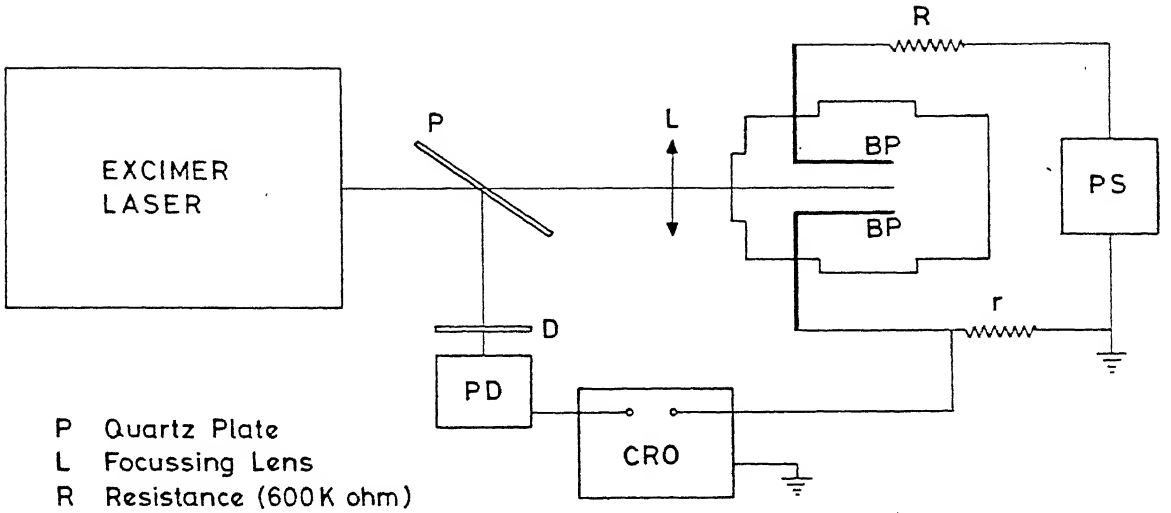

P Quartz Plate
L Focussing Lens
R Resistance (600K ohm)
PS Power Supply
r Resistance (940K ohm)
PD Photo Diode
D Quartz Diffuser
BP Brass Plates
CRO Cathode Ray Oscilloscope

Figure 1 Schematic of Experimental set up

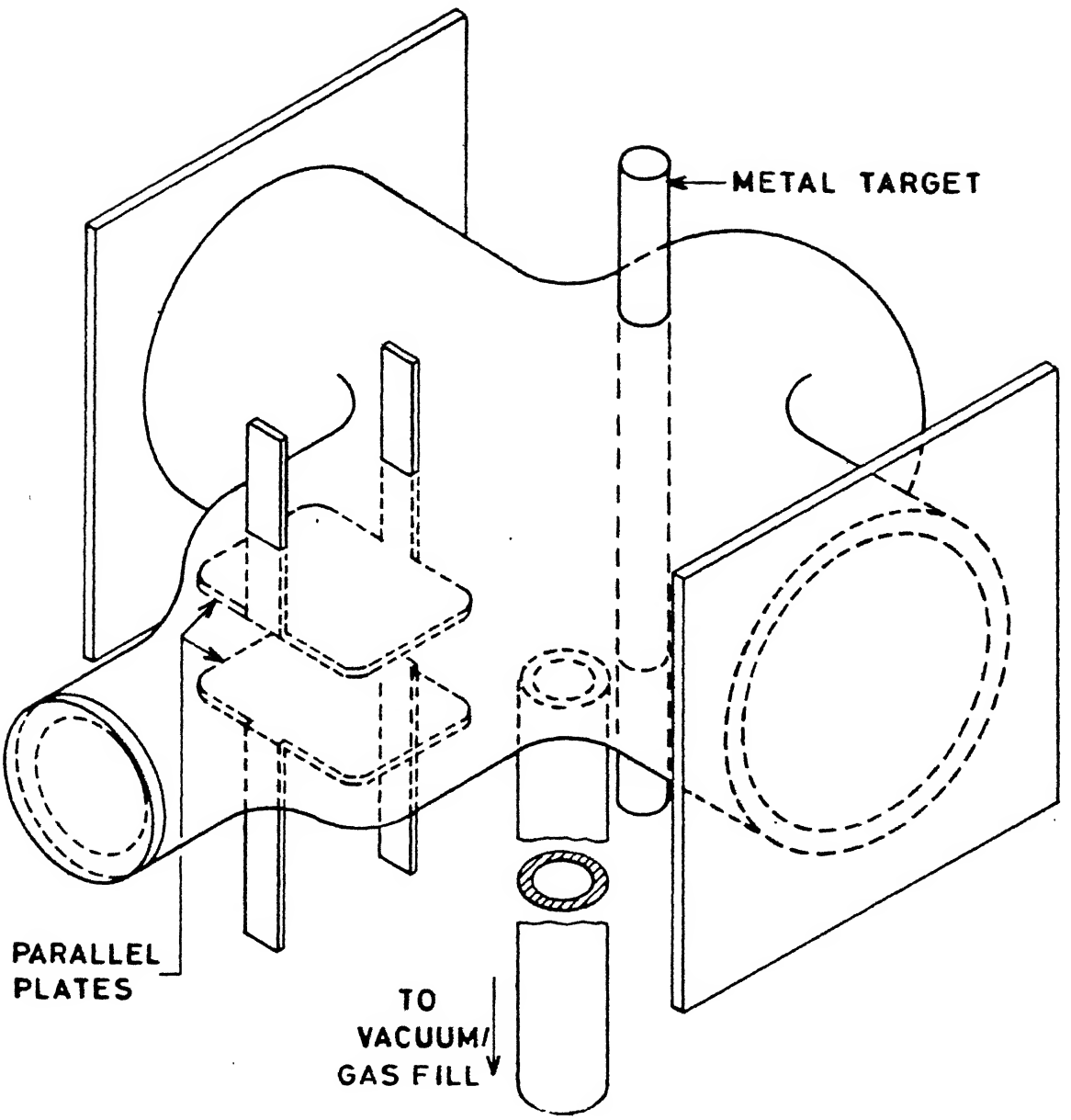

Figure 2 Schematic of the Cell.

effect of metal surface on threshold intensity of gas breakdown, an additional metal target was introduced as shown in Figure 2. The distance between the metal surface and the center of the electrodes was kept at 25 mm. Discharge cell was connected to the vacuum system and gas filling arrangement through stop cocks. The vacuum system consisted of an oil diffusion pump and rotary pump. Gas filling arrangement consisted of bulbs of neon, xenon (with 1% krypton) gases and an empty glass bulb used as a reservoir for argon gas. Glass bulb was evacuated to a pressure of $<10^{-4}$ torr and then filled in at 9 psi of argon gas from cylinder connected to the system. Discharge cell was evacuated to a pressure less than 10^{-4} torr and filled in with the gases under investigation at the desired pressure. Pressure of the gas in the discharge cell was monitored with an oil manometer. An EG & G power supply (3.0 KV, 10mA) was used to provide static electric field. Ionization current was measured in terms of voltage drop across a resistance (r) connected in series with one of the electrodes and displayed on the storage oscilloscope (100 MHz, TS 8123, Iwatsu, Japan). Ionization current of the order of 10^{-8} Amp was considered to be the breakdown current [63].

We have used Lumonics model TE 861 M-2 excimer laser [80]. The laser was operated as XeCl laser (308 nm) delivering upto 60 mJ in 25 ns pulse at 10 pps. The appropriate proportions of

Xenon (39 torr) and HCl (16 torr) gases with helium (balanced to 50 psi) as buffer gas were filled and mixed in the discharge channel. The stable resonator cavity is formed by an aluminium coated reflector (rear optic) and a quartz output coupler (front window), mounted at the ends of the discharge channel. With one filling of gases, laser used to operate at nearly constant energy for 7-8 hours after which it starts falling. The main factor involved in loss of energy during a run in these kind of lasers is the gradual disappearance of HCl as the laser operates. This was partially compensated by the judicious addition of a small amount of HCl. For all the studies, laser was operated at 10 pulses per second(pps). The laser pulse was recorded using a photo multiplier tube (PMT) (1P28 Hamamatsu, Japan) with 50 Ω termination through a monochromator. Oscilloscope trace of the laser pulse (FWHM ≈ 25 ns) is shown in Figure 3. The energy of the laser was measured with a Gen Tec joule meter (ED 200), by placing the joule meter in the path of the main beam.

Preliminary studies of metal plasma [78] were performed in a metallic chamber containing the target evacuated to a pressure less than 10^{-2} torr. In order to avoid crater formation the target was rotated at approximately 1 rotation per minute with an external motor. The studies on metal plasma in presence of background gas were performed in the discharge cell

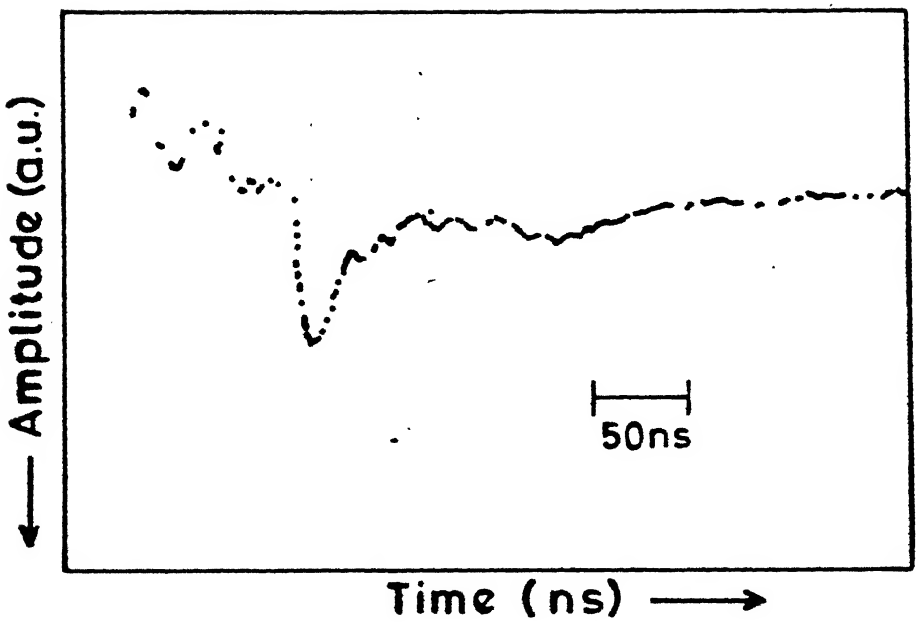

Figure 3 Oscilloscope trace of laser pulse

containing the target, similar to as shown in Figure 2. In this case, the target was exposed to laser radiation only for a small interval of time so as to avoid the effect of crater formation on the extent of metal plasma. The schematic of the experimental set up used for both the cases is shown in Figure 4. The laser radiation was focused on to the target to a focus spot of ~ 250 μm and a bright metal vapor plasma was formed. This plasma was focused on to the entrance slit of the monochromator (HRS 2 Jobin Yvon, France) with a lens. The output from the monochromator was detected with a PMT and displayed on the oscilloscope or recorded on the strip chart recorder.

A Microprocessor Controlled Scan System (MCSS) was developed [81] and used with the monochromator to scan the spectrum of radiation emitted from metal plasma. Block diagram of the microprocessor controlled scan system (MCSS) developed is shown in Figure 5. The Monochromator (HRS 2 Jobin Yvon, France) consists of a grating (1200 grooves/mm) which is to be rotated with predetermined speeds to scan the spectrum. We use a four phase stepping motor [82] (provided with the monochromator), with 200 steps, each step corresponds to 0.02 Å on the monochromator display. Stepping motor used has the characteristics that step angle is small [step angle= $\frac{360}{\text{step number}}$]; motor rotates through a predetermined step angle in response to a pulse signal and come to rest

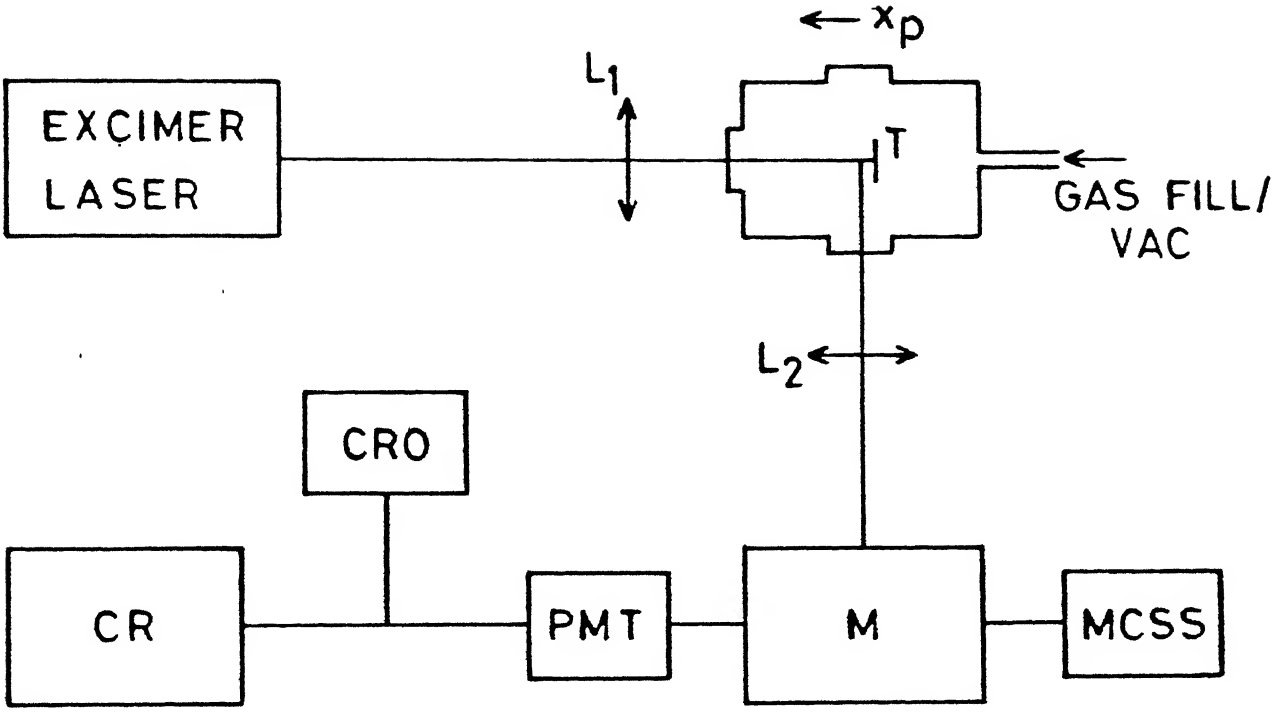

L_1 & L_2 – Lens
M – Monochromator
MCSS – Microprocessor Controlled Scan System
PMT – Photomultiplier Tube
CR – Chart Recorder
CRO – Cathode Ray Oscilloscope
T – Target

Figure 4 Experimental set up for Metal Plasma Studies.

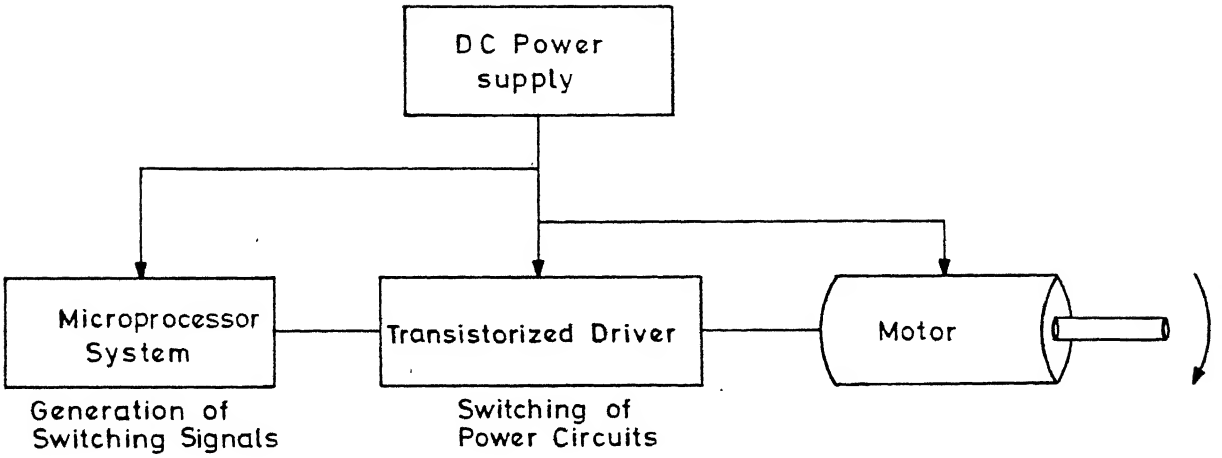

Figure 5 Block diagram of the MCSS

at precise position. It has high torque to inertia ratio so that it has a quick start/quick stop response to input/last pulse. The rotation of the motor can be controlled in units of the step angle by the switching process. If the switching is done in sequence the motor rotates with a stepped motion. The average speed of the motor can also be controlled by the switching processes. A microprocessor system based on 8085A processor chip was used to control the average speed of the motor. Software was developed to select scanning speeds, upper and lower boundaries of the scan, and forward/reverse scan. A subroutine can be added for digitizing the analog output from a PMT using interfacing electronics. The power supply used for the MCSS and motor should be free from any kind of ripples. A regulated power supply (5V, 3A), for the microprocessor system and motor was assembled using UA 323 chip; any unwanted pulse can destroy the program of the microprocessor system.

The stepping motor moves when pulse trains are applied to it in a proper sequence. The motor under consideration receives pulses programmed [83,84] through the microprocessor such that only two phases of the motor are energized at a time. The change of excitation from one pair of excitation coïl to other rotates the motor by one step. A flow chart of the program developed is given in Figure 6.' By defining the upper and lower positions of scan it was possible to scan the spectrum in

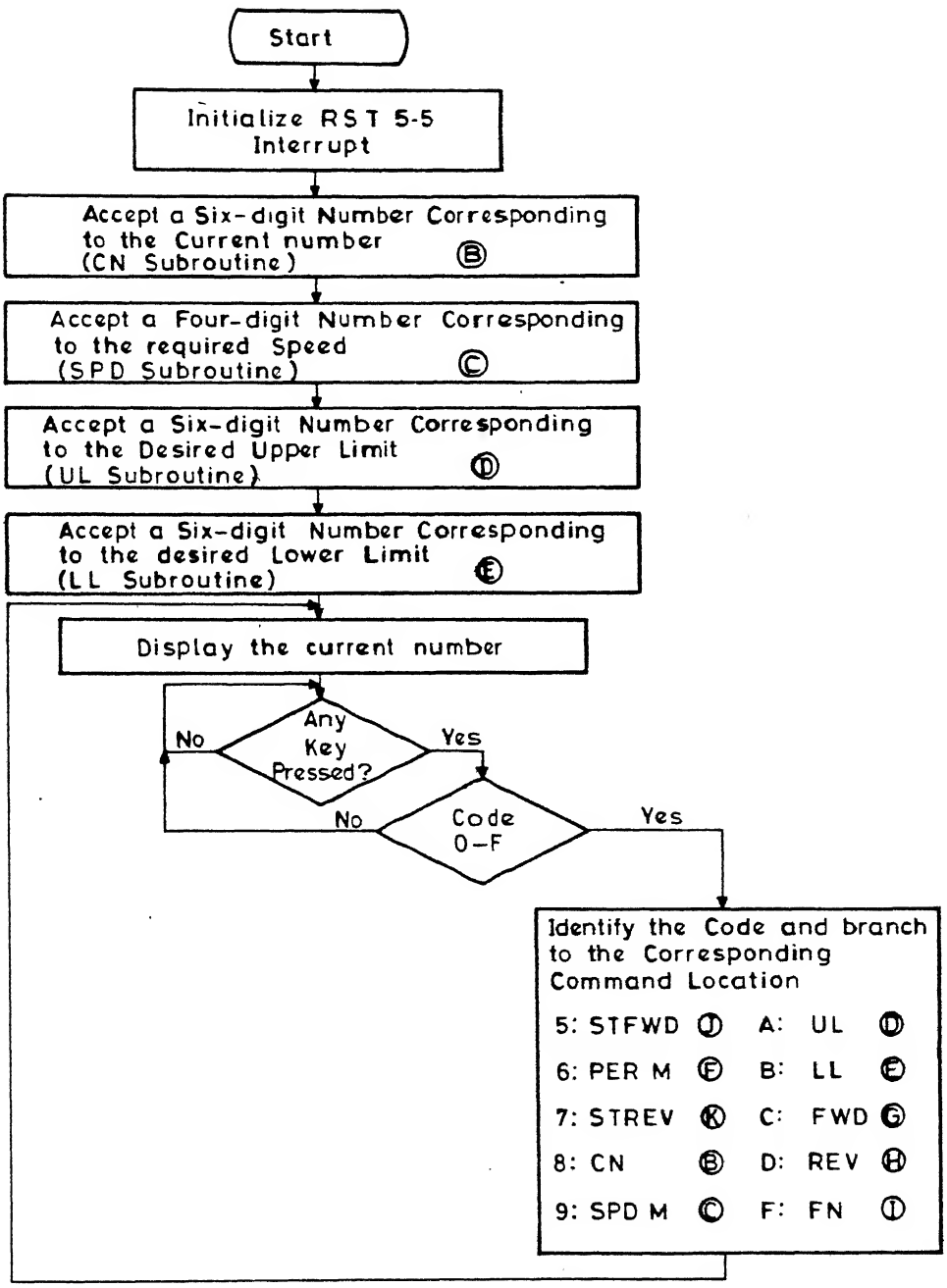

Figure 6a Flow chart of the Main program.

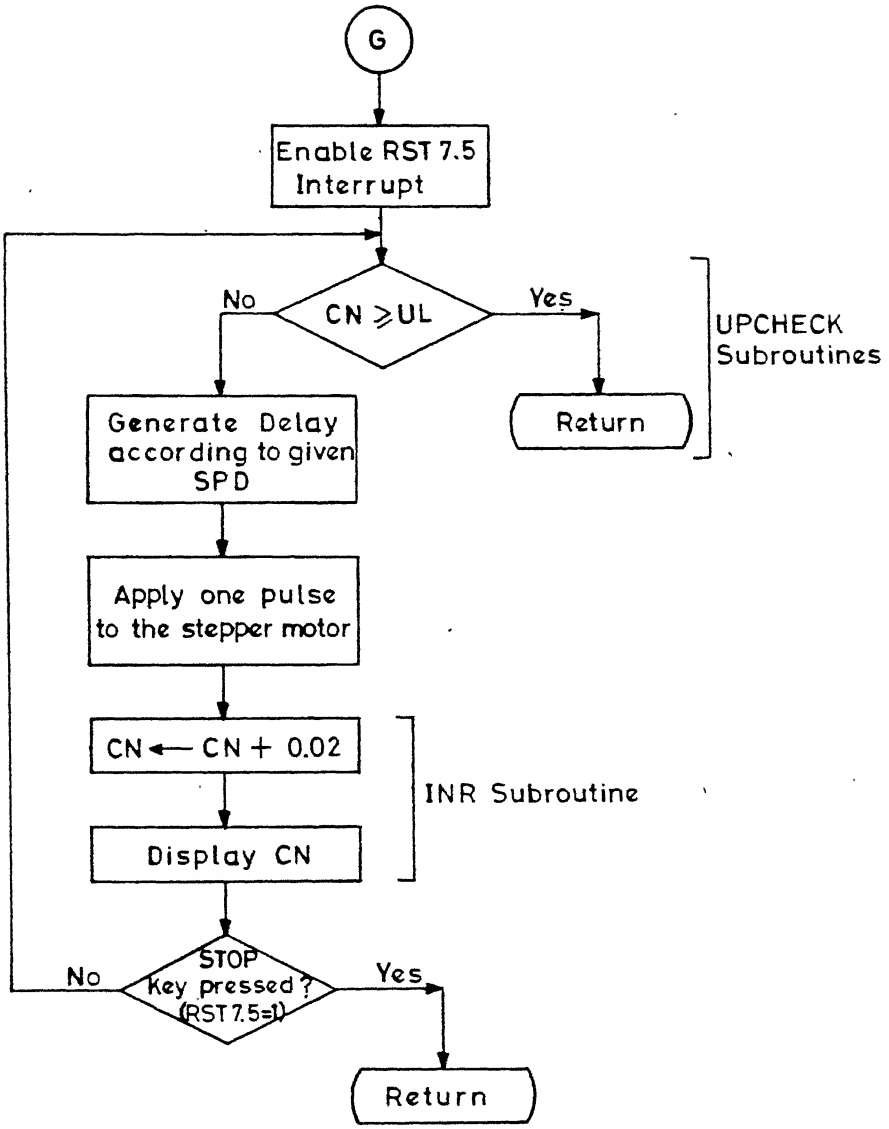

Figure 6b Flow chart of FWD subroutine

forward (or reverse) direction at speed ranging from 0.02 A/min to 300 A/min with the stepping motor used in our set up. The main program to move stepping motor is given in Figure 6a. Subroutines being used are abbreviated as:

STFWD - Step Forward, PERM - Period: Main, STREV - Step Reverse, CN - Current Number, SPDM - Speed: Main, UL - Upper Limit, LL - Lower Limit, FWD - Forward, REV - Reverse, FN -Final Number. Various subroutines are identified by alphabet in circle and command location on microprocessor system on the left, for example C: FWD(G) reads command location C, subroutine Forward being identified by G.

The microprocessor system used to control the motor is a low cost Inlet 8085 A based eight bit microprocessor system (Microfriend-I) manufactured by M/s Dynalog Micro-system, Bombay (India). Figure 7 is a functional block diagram of the microprocessor system (Microfriend-I) showing the common communication path between various components through the data bus. The Central Processing Unit (CPU) is used along with Programmable Peripheral Interface (PPI) Chip 8255A. The PPI chip 8255A is used for outputting the pulse sequence to move the stepper motor. The 8255A has three 8 bit ports, namely A, B and C. Built in subroutines of the monitor [83] are used to accept the input data from the monitor keyboard and to display output data and other information on the kit LED Display. Sequential

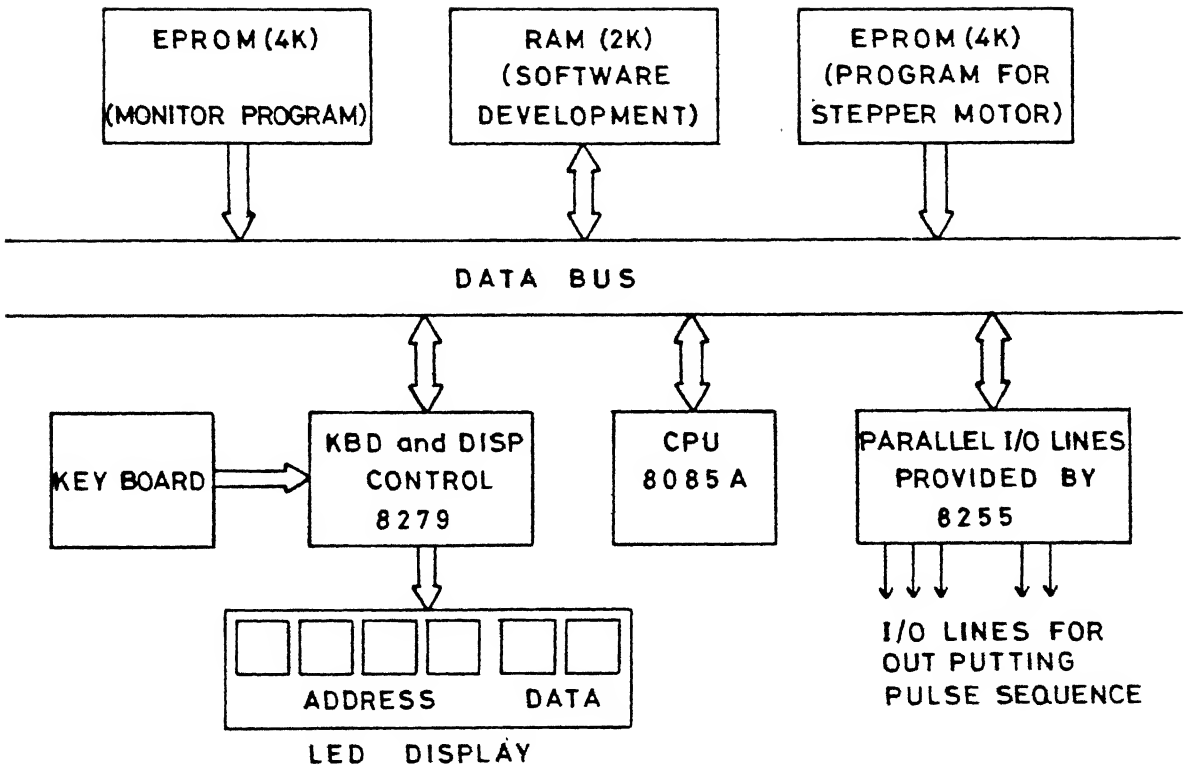

Figure 7 Functional block diagram of the microprocessor system (Microfriend-I).

pulses coming out from port B of PPI are used for driving stepping motor. Since microprocessor peripheral can support a current of the order of a few mA, whereas the current rating of the motor to be driven is usually high (~ 1 Amp), an external driver circuit as shown in Figure 8, was developed.

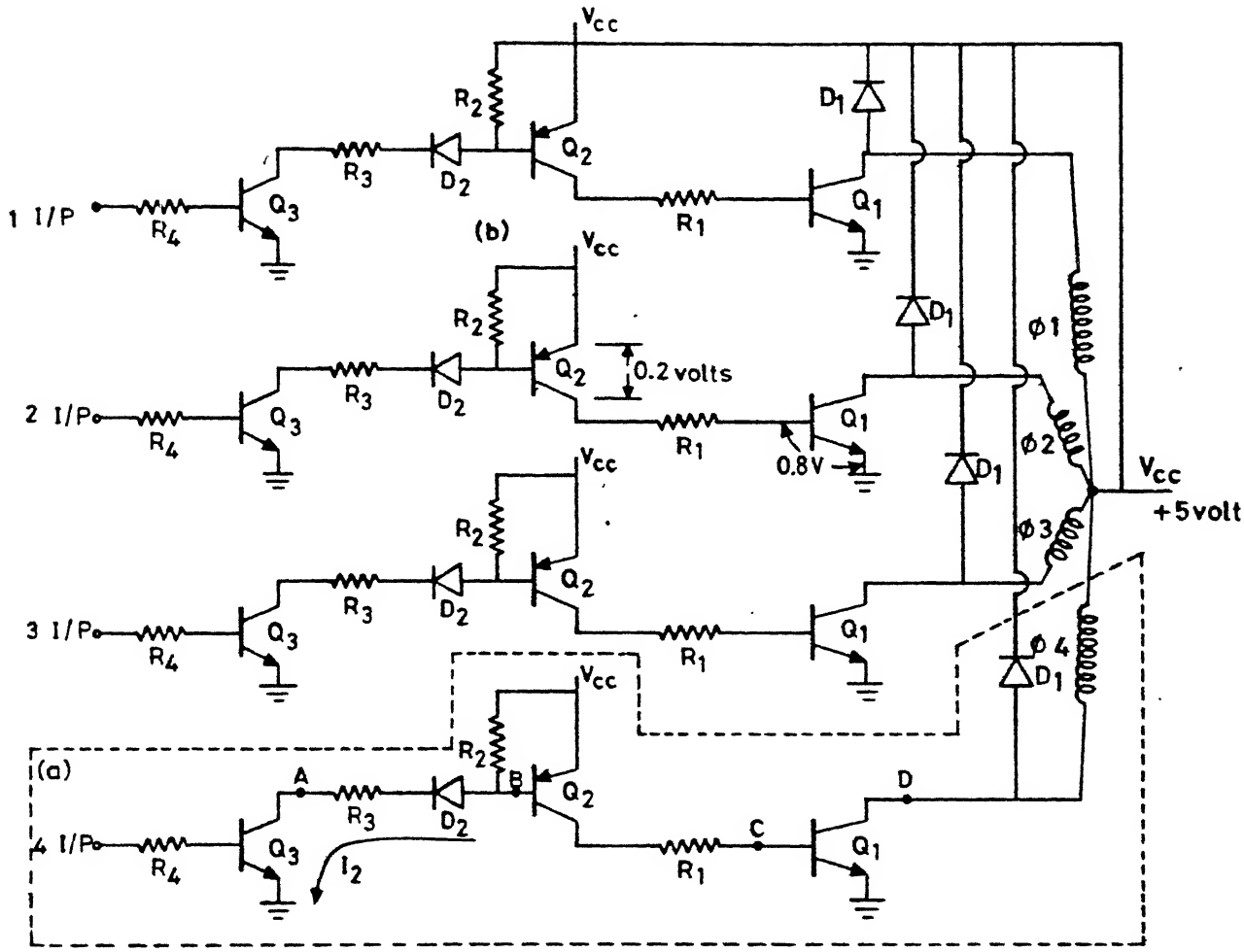

Figure 8 Driving Circuit for Stepping Motor.

CHAPTER 3

Laser Induced Gas Breakdown in the Presence of Static Electric Field

Introduction

Gas breakdown can be observed in the presence of (a) static field only, (b) high intensity laser beam only and (c) laser beam and static field. Case (a) has been extensively studied [63]. Many researchers [3,5,36,85,86] have studied the case (b) and studies are still going on. In case (c), partial excitation of the gas by an applied static field permits the observation of breakdown by low intensity light which could otherwise not be observed at such low intensities [58,60,61]. Recently there have been reports on the gas breakdown with low intensity laser beam in the presence of a static electric field, not sufficient for continuous self sustained discharge [64,87,88]. Kopeika et al [61] used Hamamatsu R702 (argon) gas-filled phototube as a discharge tube and static field was applied to the discharge tube to operate in Townsend discharge region. Tungsten lamp with a monochromator was used as a light source of low intensity. Low intensity lasers have also been used [64,87] as a light source for the studies of case (c). It was observed [61] that the breakdown effects using low intensity light in presence of static field are similar to that observed in case (b). Tulip et al [62] observed that threshold for laser-induced gas

breakdown is influenced by static electric field. However, there has been no report showing variation of k_o, the number of photons involved to breakdown the gas, with static field. A detailed study was undertaken to understand the behavior of laser induced gas breakdown in presence of static field. Variation of k_o for Ne, Ar and Xe gases with static electric field in a simple discharge cell using an excimer laser are reported for the first time [65].

Experimental set up

Experimental set up used is described in Chapter 2. A schematic layout is shown in Figure 1. An excimer laser (308 nm) delivering upto 60 mJ in 25 ns, at 10 pps, was focused with a quartz lens (f=12 cm) in the center of a discharge cell. The two electrodes are separated by a distance of 6.5 mm. The cell was evacuated to a pressure of $\leq 10^{-4}$ torr and then filled in with the gas to be investigated at the desired pressure in the range of 0.2 - 24.0 torr. An EG & G power supply was used to provide transverse static electric field (TSEF). To get clean laser beam an aperture of 30×10 mm^2 was placed in the path of the main beam. Laser power was monitored by using reflection of the main laser beam from a quartz plate, with the help of a photodiode (SGD 100A, EG & G USA). The photodiode signal was calibrated with an energy meter (ED 200, Gen Tec Inc, Canada). Laser energy was varied either by reducing the firing voltage of the laser

(always above threshold voltage) or by inserting glass plates in the path of the main laser beam. TSEF was adjusted such that there is no ionization signal with either static field only or laser radiation alone. Ionization current of the order of 10^{-8} Amp measured in terms of voltage across a resistance r (940 KΩ) connected in series with one of the electrodes was considered as breakdown current [63] and the signal was displayed on the storage oscilloscope (TS 8123 Iwatsu, Japan). Every point on the figures to follow is an average of five points.

Results and Discussions

Figure 9 shows the dependence of transverse static electric field threshold to get breakdown signal with and without laser radiation, as a function of pressure of various gases under investigation at constant laser energy. Behavior is similar to that of Paschen's curve [89]. Figure 10 shows the dependence of laser energy threshold on gas pressure at constant TSEF (transverse voltage being 16 volts for neon and 65 volts for argon) to get breakdown signal. These curves also follow the trend of Paschen's curve. At very low pressures (p) the collision frequency (ν_c) is low, ($\nu_c \alpha$ p), sufficient ionization can only be maintained by increasing the probability of ionization at each collision (consequently the electron velocity) and thus electric field should be high. Hence

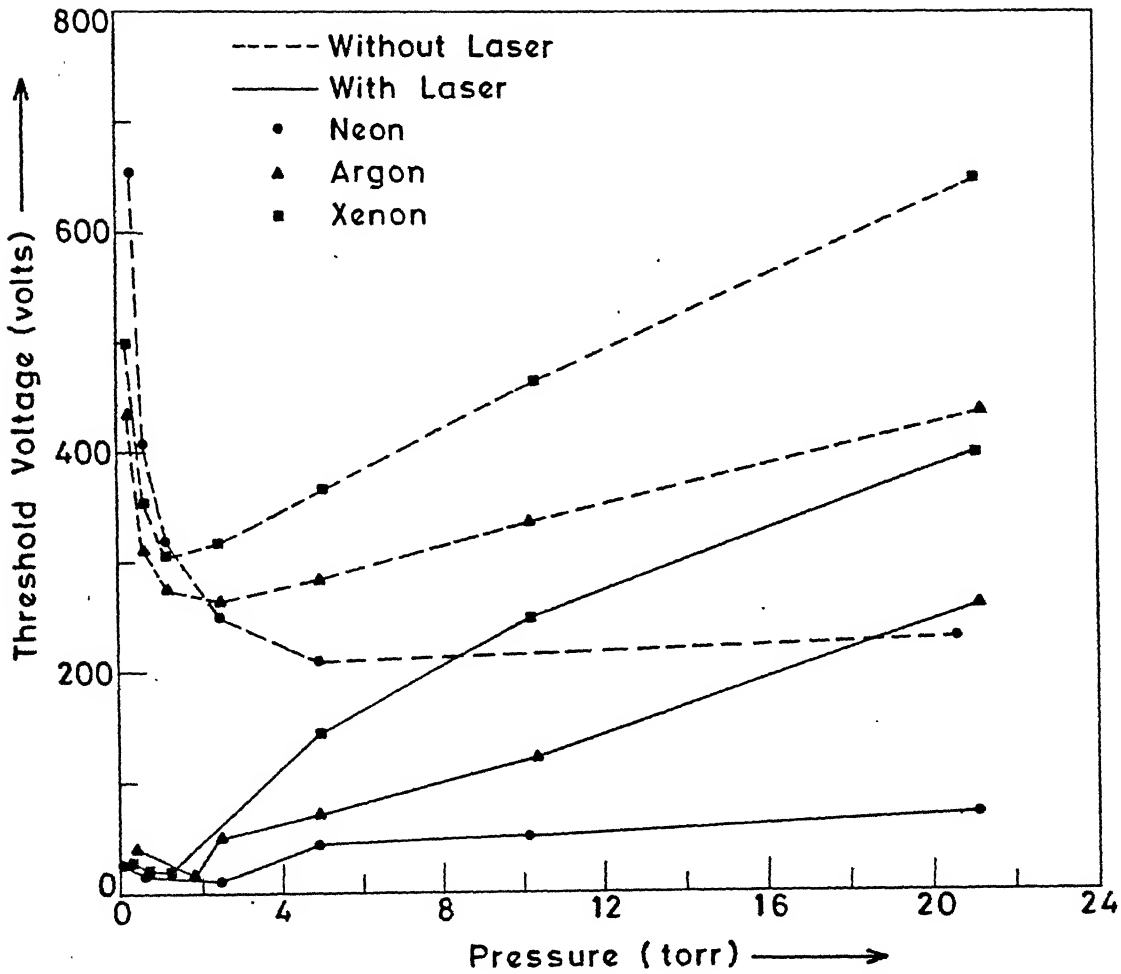

Figure 9 Dependence of threshold transverse voltage on the gas pressure with and without Laser Field.

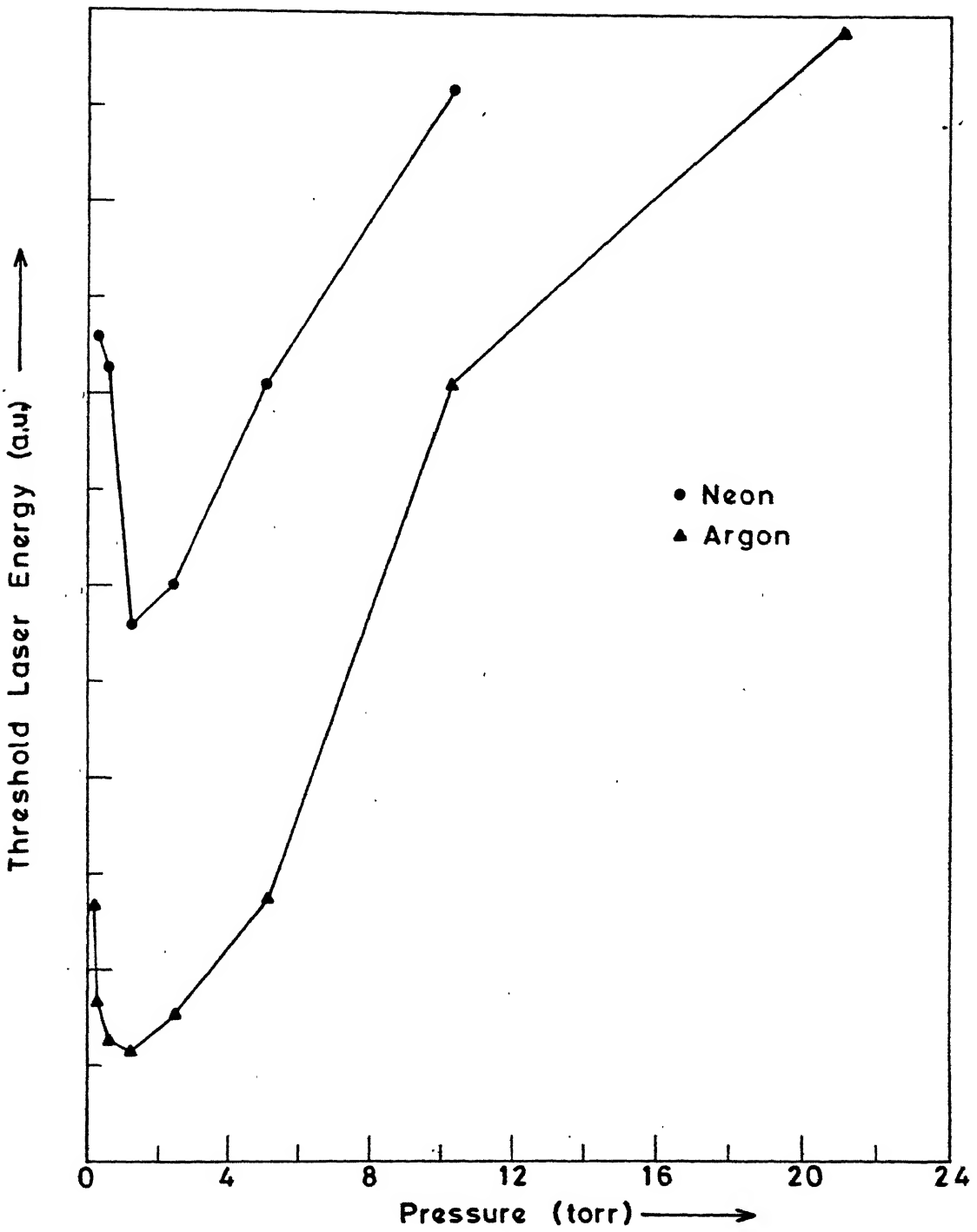

Figure 10 Dependence of threshold laser energy on the gas pressure in the presence of transverse voltage

threshold voltage increases as p decreases, for very low p at a fixed separation (d) between plates. On the other hand, at high pressures the collision frequency is high and the rate of energy loss is correspondingly high, while the energy gained per free path is low (mean free path $\alpha \frac{1}{p}$) unless the field is correspondingly high. Hence threshold voltage increases as p increases for a given d. Thus the Paschen's curves show a minimum threshold voltage to breakdown gas when pressure increases from a very low value of p.

Figure 11 shows variation of ionization current with TSEF for Ne Ar and Xe at a pressure of 5 torr and 21 torr .This shows that laser induced ionization current increases with the increase in TSEF at constant laser energy. As the static field increases, the probability of excitation/ionization increases. However, for large enough voltage static discharge occurs between the electrodes. Our results are in agreement with Tulip and Seguin [62].

Figure 12 shows the variation of ionization current with laser energy at constant TSEF (transverse voltage is 150 volts) for Ne and Ar at a pressure of 1 torr. The ionization current increases with the laser energy, here excited atoms due to static field are photoionized with laser field. The increase in laser energy (photon flux, number of photons/sec cm^{-2}) increases the probability of photoionization of excited atoms and hence

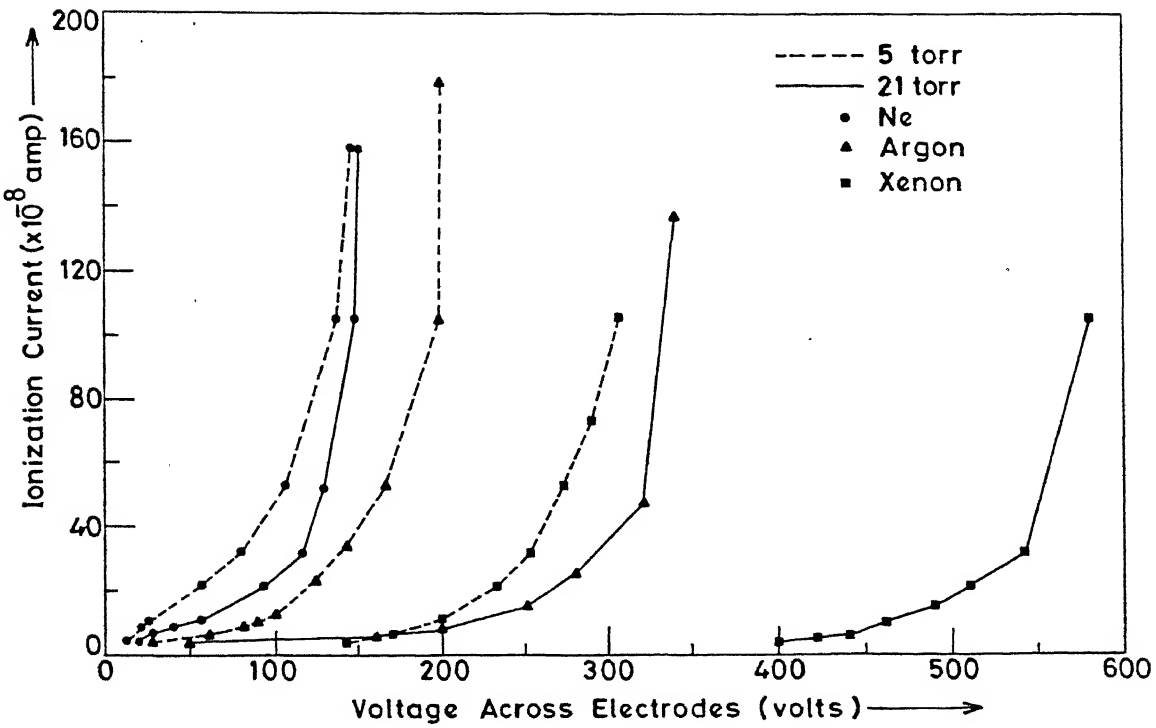

Figure 11 Variation of ionization current with transverse voltage at constant laser energy

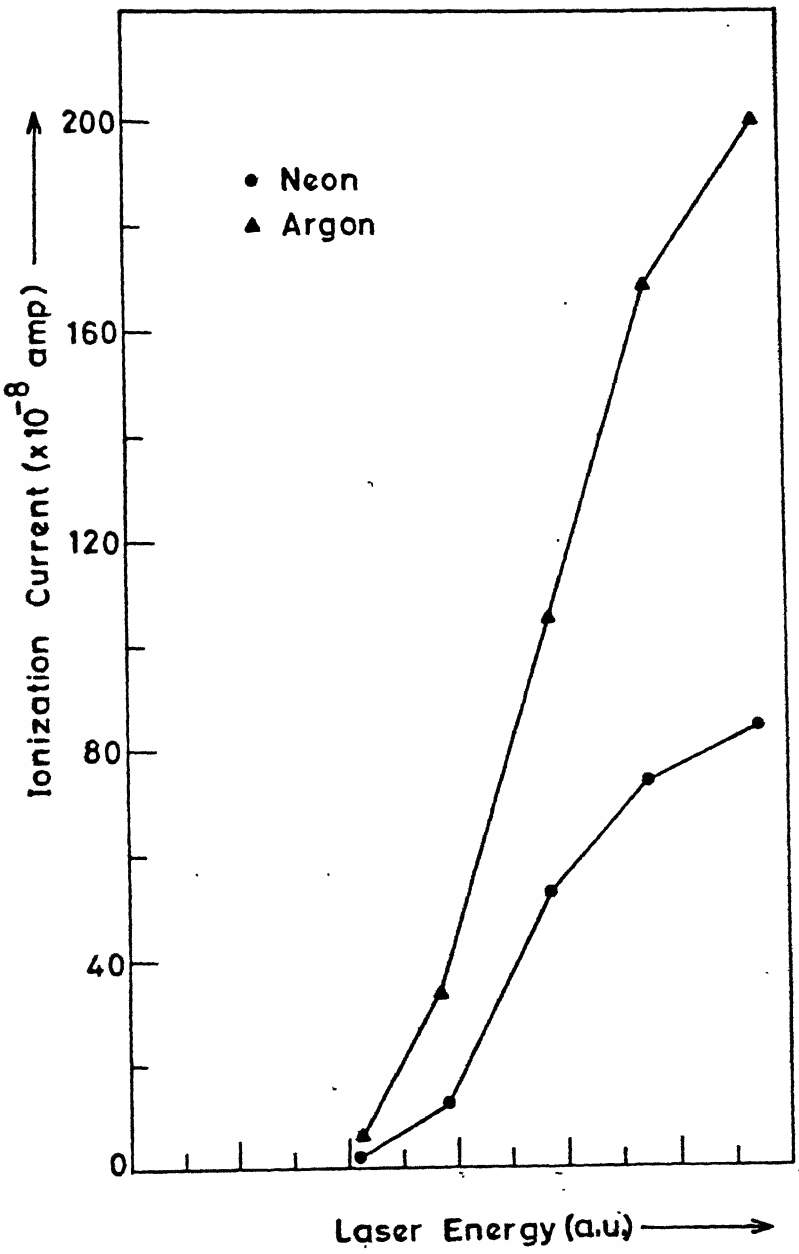

Figure 12 Variation of ionization current with laser energy at constant TSEF

the ionization current increases. Results are in agreement with earlier report [64].

The ionization probability is described by the power law, $W = A_i I^k$, {eqn (1)} where $k = < E_i/E_p >$, defines the number of photons required to ionize the gas, which may be different from k_o, the number of photons actually involved to ionize the gas. Figure 13 shows the variation of Log (ionization current) with Log (laser energy) for Ne and Ar at the pressure of 1 torr in the presence of TSEF. Initially the ionization current increases very rapidly with increasing laser energy. The slope of the curve gives the experimental value of k_o, mentioned on the curve for various values of static electric field. It is observed that k_o decreases with the increase of static electric field. The decrease in k_o with the increase in static field may be due to increase of probability of excitation/ionization leading to higher excited states. When the laser energy increases beyond a certain value the ionization current proceeds less rapidly and shows a turning point. Beyond the turning point the slope of the curves lies between 1 and 2, in agreement with earlier report [3] on gas breakdown using high power lasers. The turning point which was observed for both the gases investigated, according to Agostini et al [3], may correspond to total ionization of all the atoms present in the interaction volume. The increase in the ionization current observed after this saturation point

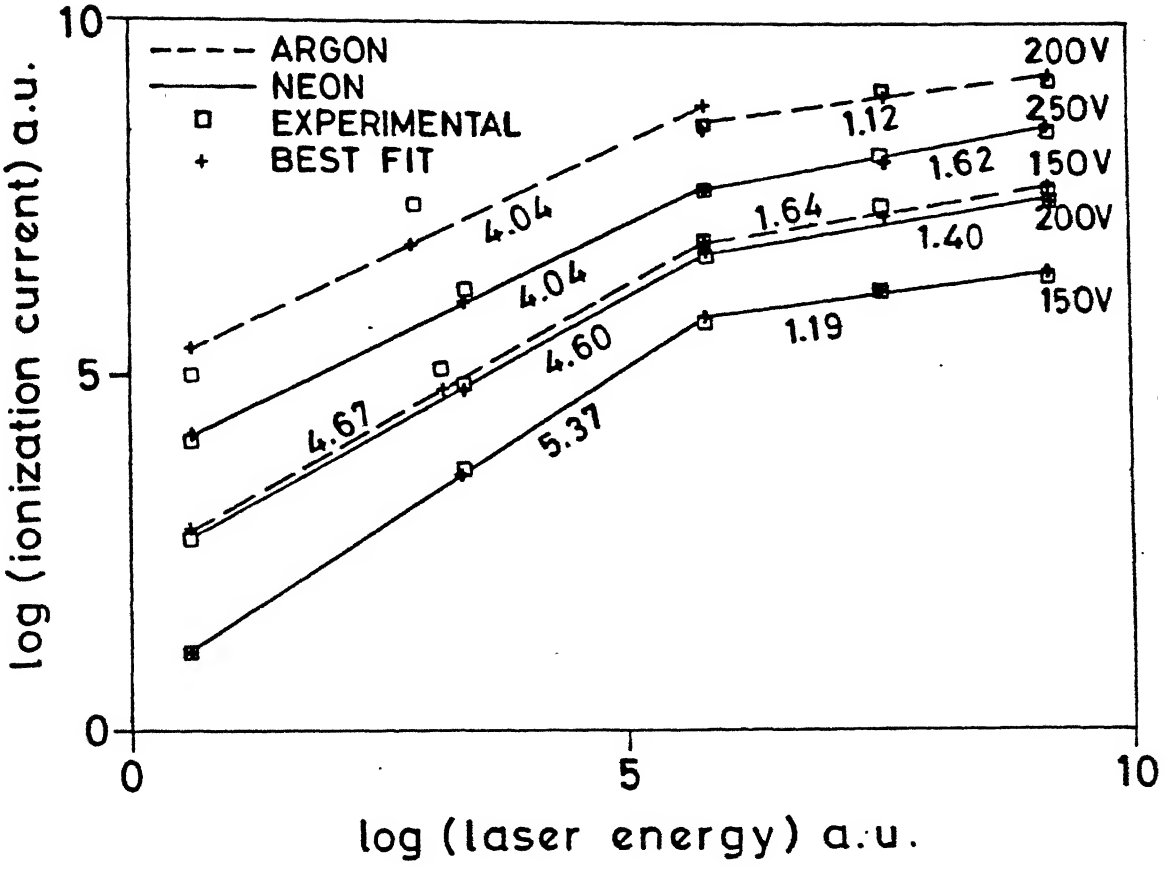

Figure 13 A plot of Log (ionization current) Vs Log (laser energy) in arbitrary units.

corresponds to ionization of atoms in the immediate neighborhood of the interaction volume. The slope depends only on the optical characteristics of the focusing system [3]. Thus our results [65] are similar to that observed with high power lasers [3]. In our case ionization is a two step process, initially excitation through collision of atoms with electrons due to TSEF followed by photoionization due to laser field. In the case of high power lasers ionization is due to simultaneous absorption of large number of photons. On comparing the value of k_o for Ne and Ar gas in Figure 13, we find that k_o is more for Ne than that for Ar gas under similar conditions of pressure and static field. It is expected since the ionization energy of neon is more than that of argon.

In conclusion laser induced breakdown of Ne, Ar and Xe gases at various pressures with low power excimer laser in the presence of a transverse static electric field is reported. Results are similar to that observed using high power laser alone. Ionization of gases is proposed to be a two step process, initial excitation being through collision of atoms with electrons due to static electric field followed by photoionization in presence of laser. We find that k_o decreases with the increase of static electric field.

CHAPTER 4

LASER INDUCED BREAKDOWN OF ARGON GAS NEAR METAL SURFACE

Introduction:

First observation of low threshold optical breakdown of gases at the surface of a target was reported [66] in 1972 using CO_2 lasers. Breakdown of air at the surface of a metal using low power laser was reported [67] and explained on the basis of thermal processes which accompany optical breakdown. It was observed that the presence of a precursor plasma [69] decreases the threshold intensity for breakdown of atomic and molecular gases. Short wavelength radiation [71-73] emitted from the metal plasma was also found to reduce the threshold intensity for breakdown of gases. In these reports CO_2 laser was focused on to the metal surface and decrease of threshold laser energy was observed by monitoring breakdown signal using the photomultiplier tube. The decrease in threshold laser energy was attributed either to thermal process [67] or presence of metal plasma itself [71-73]. However, there has been no report, to the best of our knowledge, on the effect of the threshold laser energy required to breakdown the gas by photoelectric emission from the target surface using short wavelength lasers. Current densities of 500 Amp/cm^2 has been observed [77] as a result of five photon surface photoelectric effect in gold using 10 ps Nd:Glass laser ($\sim$ GW/cm^2). We undertook a detailed study to find

out the mechanism of laser induced breakdown of argon gas near metal surface in the presence of static electric field. We report [74] that the photoelectric emission from the copper target reduces the threshold laser energy required to breakdown argon gas.

Experimental Setup

Details of the experimental set up are given in Chapter 2. Experimental arrangement is similar to that used in Chapter 3, except that now discharge cell contains a copper target at a distance of 25 mm from the center of the electrodes as shown in Figure 2. The plates separation being 6.5 mm. The cell was evacuated to $\leq 10^{-4}$ torr and then filled in with argon gas at desired pressure in the range of 0.5 torr - 22 torr. To start with, laser is focused on to the copper target, a bright green plasma [78,79] is observed, this position of best focusing of lens is referred to as x = 0. The irradiation on to the target and hence the extent, size of the plasma is reduced by moving the lens away from the copper target on the same optic axis (x increases in -ve direction i.e. away from the target). We define a defocussing parameter, x, as the position of the lens along the laser axis for the present studies. Transverse Static Electric Field (TSEF) applied across the electrodes was adjusted such that there was no ionization current signal with either static field or laser radiation alone.

Results and Discussions

We studied the variation of ionization current with defocussing parameter viz various values of x. At x = 2 mm and laser energy 6.4 mJ, we observe a double peaked voltage pulse as shown in Figure 14a. The first peak is identified due to the breakdown of argon gas and the second peak as the signal due to copper ions which is delayed with respect to first due to time of flight of copper ions. As x increases, the size of the plasma and the amplitude of the second peak decreases. At x = 8 mm, copper plasma is not visible and second peak vanishes completely as shown in Figure 14b. Our investigations in the following correspond to the ionization current at $x \geq 8$ mm.

Figure 15 shows the dependence of laser energy threshold, normalized to the maximum laser energy, on argon gas pressure with and without the copper target at constant transverse static voltage of 40 volts at x = 8 mm, to get breakdown signal [65]. Observed behavior is similar to that of Paschen's curve [89]. It is observed that the threshold laser energy required to breakdown argon gas at any specific pressure decreases in the presence of a metallic target. Figure 16 shows the variation of ionization current of argon gas with defocussing parameter, x, for different values of laser energy in the presence of copper target at argon gas pressure of 1.2 torr and transverse static voltage of 150 volts. The

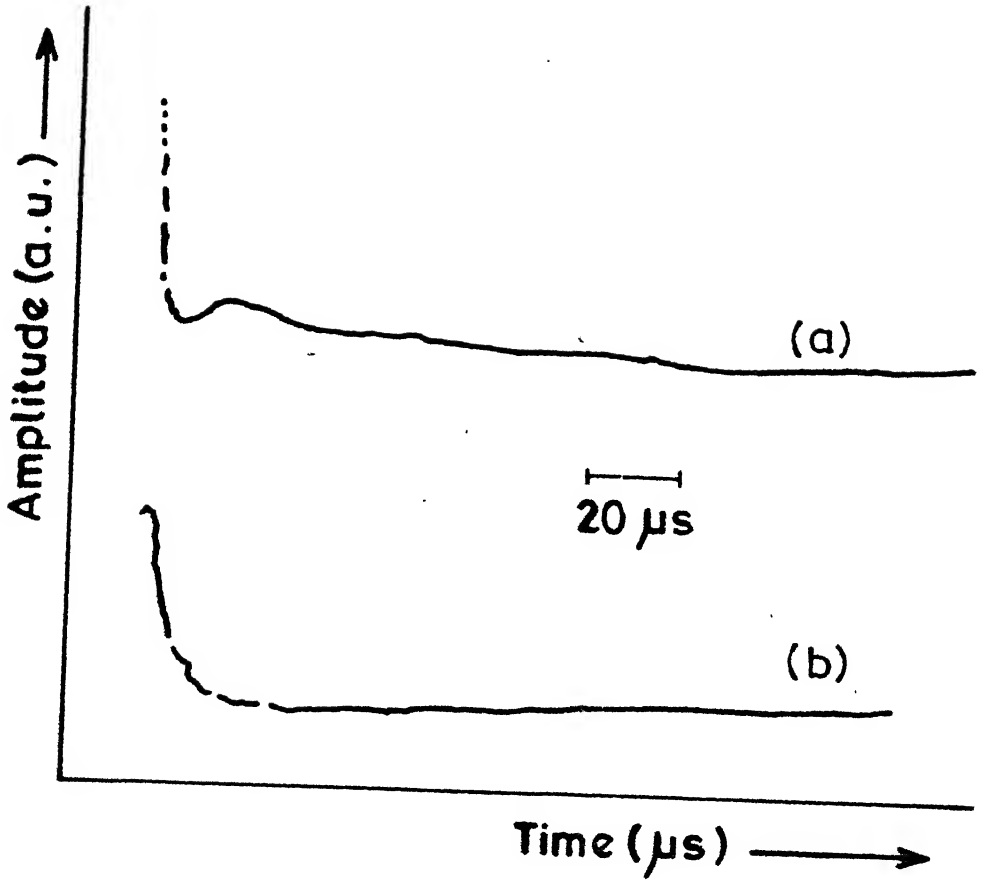

Figure 14 Ionization current pulse (a) at x = 2 mm (b)at x = 8 mm.

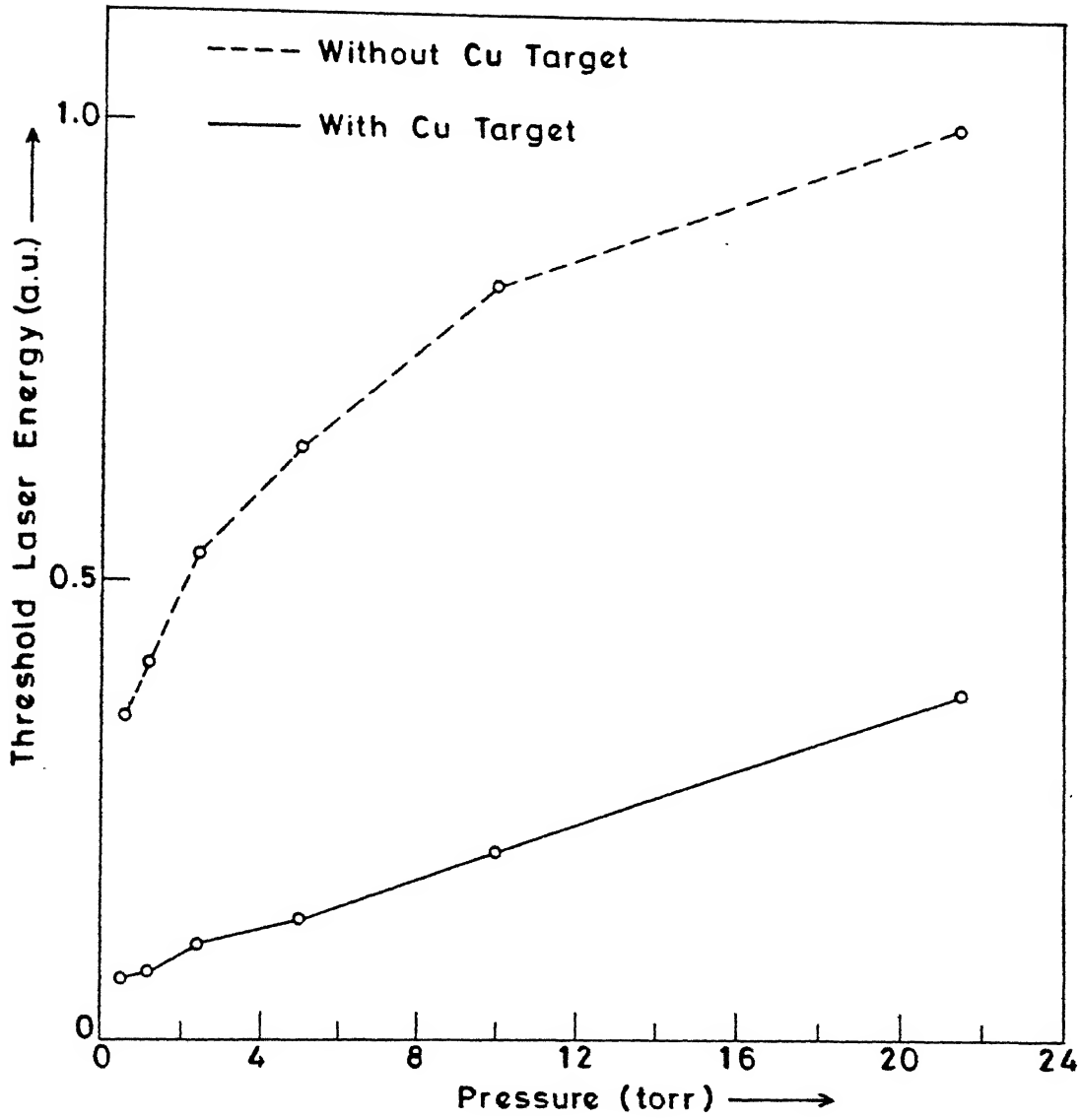

Figure 15 Dependence of threshold laser energy on the argon gas pressure with and without copper target at constant TSEF.

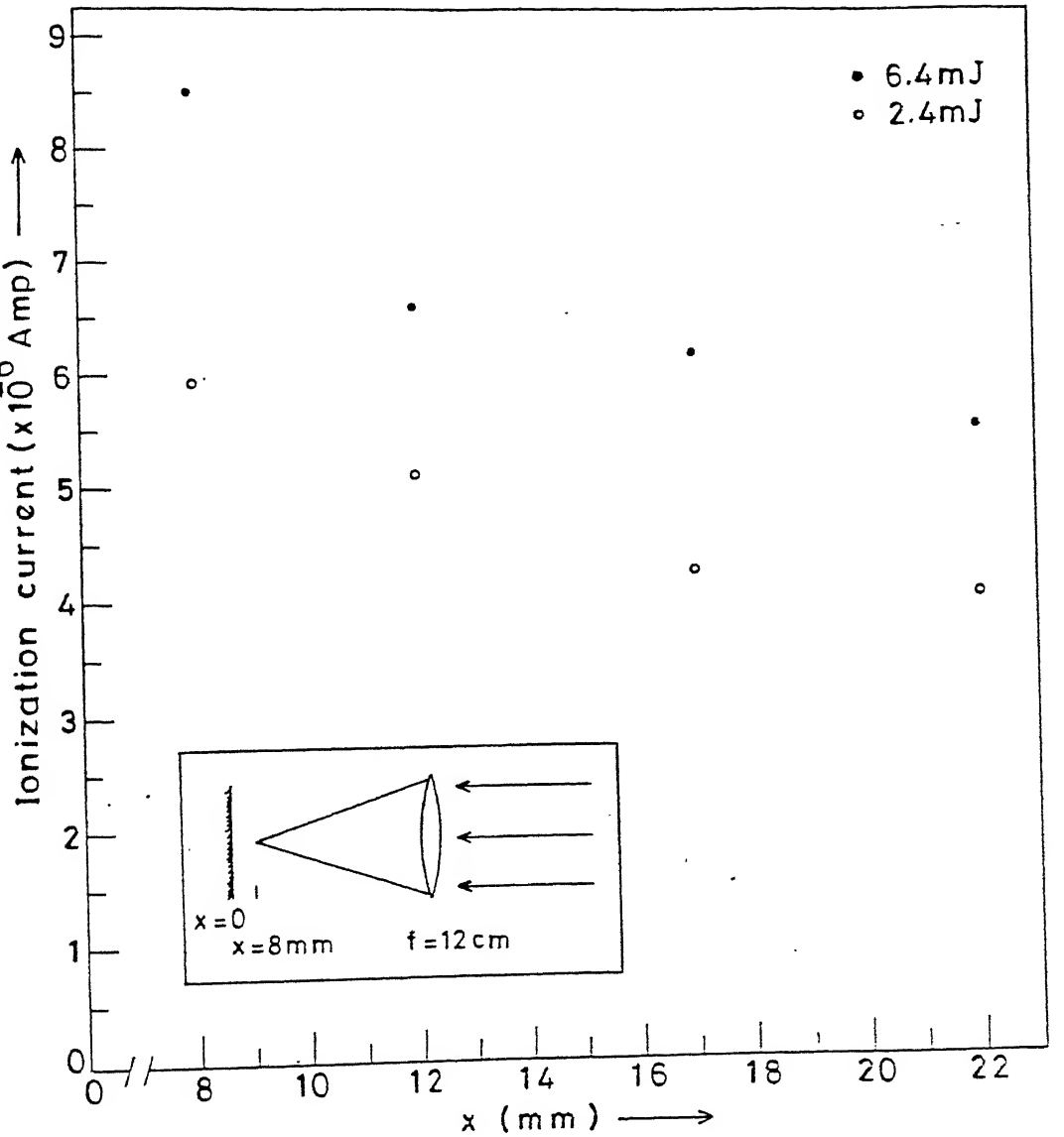

Figure 16 Variation of ionization current of argon gas with defocussing parameter, x, at constant TSEF.

ionization current decreases with increase in x, because the irradiation on copper target and hence the probability of electron emission decreases with increase in x. To find the initial source of electrons helping in ionizing the argon gas, we estimate the electron current density due to two fundamental processes viz thermionic emission and multiphoton photoelectric emission from copper surface.

First let us look at the thermionic effect. The current density j_{th} of electrons emitted from a metal surface because of thermionic emission at surface temperature T_s is given by the Richardson's equation [90],

$$j_{th} = A_{th} T_s^2 \quad \exp(-E_\phi / K T_s) \qquad (4).$$

where A_{th} is a constant given by $\dfrac{4 \pi m K^2 e}{h^3} = 120$ Amp/cm^{2}deg.^{2} E_ϕ is work function of the metal and K is Boltzmann's constant.

Consider the laser induced transient temperature T(z,t) where z defines the surface depth. This obeys heat diffusion equation [91],

$$\frac{\partial T}{\partial t} = D \frac{\partial^2 T}{\partial z^2} \qquad (5).$$

with initial and boundary conditions,

$$T(r,z,0) = T_0 \qquad \text{at } t=0,$$

$$K_c \frac{\partial T}{\partial z}\bigg|_{z=0} = -(1-R)\, I(r,z,t)\big|_{z=0} \qquad \text{at the surface, } z=0$$

where $T(r,z,t)$ is the laser irradiated target temperature with hot spot centered at $r = 0$; R, the surface reflectivity; D, the thermal diffusivity; K_c, the thermal conductivity and I, the incident laser intensity $I(r,0,t) = I_o \exp[-(r/d)^2]g(t)$ in terms of spatial gaussian dependence and temporal dependence $g(t)$. Following Lin and George [91], surface temperature $T_s(r,0,t)$ generated by a triangular pulse (gaussian or an asymmetric long tail pulse) is given by

$$T_s(r,0,t) = T_o + B(r)\, I_o\, T_1(t) \qquad 0 \le t \le a \qquad (6a).$$

$$= T_o + B(r)\, I_o \sum_{i=1}^{3} T_i(t) \qquad a \le t \le a+b \qquad (6b).$$

$$= T_o + B(r)\, I_o \sum_{i=1}^{4} T_i(t) \qquad a+b \le t \qquad (6c).$$

where $$B(r) = (1-R)\, \frac{\exp[-(r/d)^2]}{[\pi K_c^2/D]^{1/2}}$$

and $\sum_{i=1}^{4} T_i(t)$ are as defined in ref.[91]. Define the time for the

peak of laser intensity and the maximum surface temperature as $t_1 = a$ and $t_2 = aL^2/(L^2-1)$, respectively. The delay $\Delta t = t_2 - t_1$, in reaching the maximum surface temperature w.r.t. peak of laser intensity is given by $a/(L^2-1)$ with $L = (a+b)/b$ where a and b marked in Figure 17 are the parameters of the laser pulse used in our experiment. The laser pulse shown in Figure 17 was recorded using photomultiplier tube (1P 28, Hamamatsu, Japan) with 50 Ω termination. Figure 18 shows the estimated rise in surface temperature $T_s(0,0,t)$ at x = 12 mm for our experimental conditions. The corresponding estimated thermionic current density is 3.70×10^{-54} Amp/cm^2. Maximum surface temperature occurs at 35.5 ns. Maximum surface temperature and corresponding thermionic electron current density for different values of x for copper target are listed in Table 1. We have used 4.48 ev for work-function; 34.3 % for reflectivity; 4.01 W cm^{-1} ^{o}C^{-1} for thermal conductivity ; 1.19 cm^2 sec^{-1} for thermal diffusivity and initial temperature of 300 ^{o}K.

Now let us consider the contribution due to photoelectric effect [90]. Since in our case laser photon energy is 4.04 eV and work function of copper is 4.48 eV, two photon photoelectric effect is expected. Figure 19 shows the temporal behavior of the photocurrent pulse. The pulse was recorded using 50 Ω resistance. On comparing the laser pulse (Figure 17) and the photocurrent pulse (Figure 19) we observe no appreciable delay

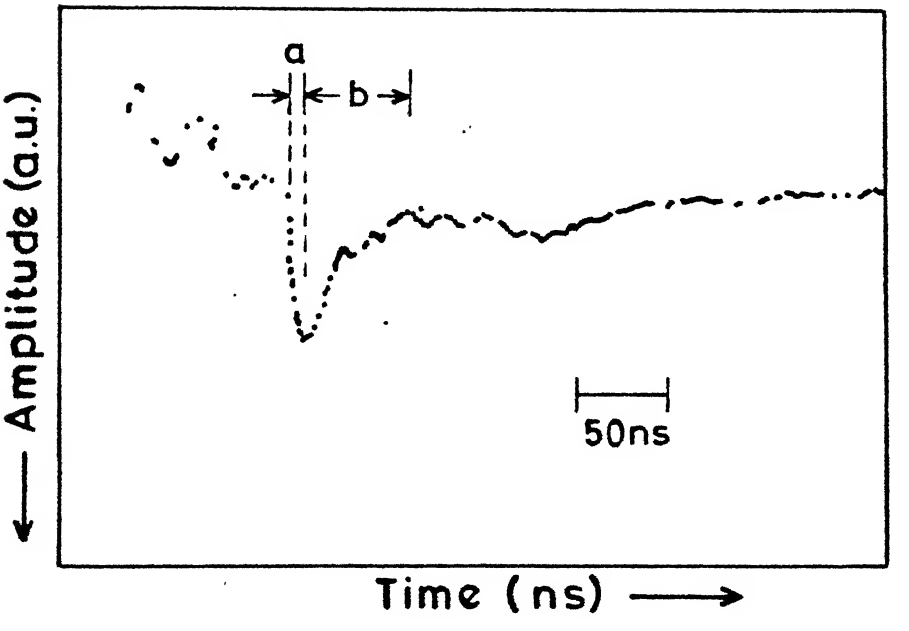

Figure 17 Oscilloscope trace of laser pulse showing parameters a and b as discussed in the text

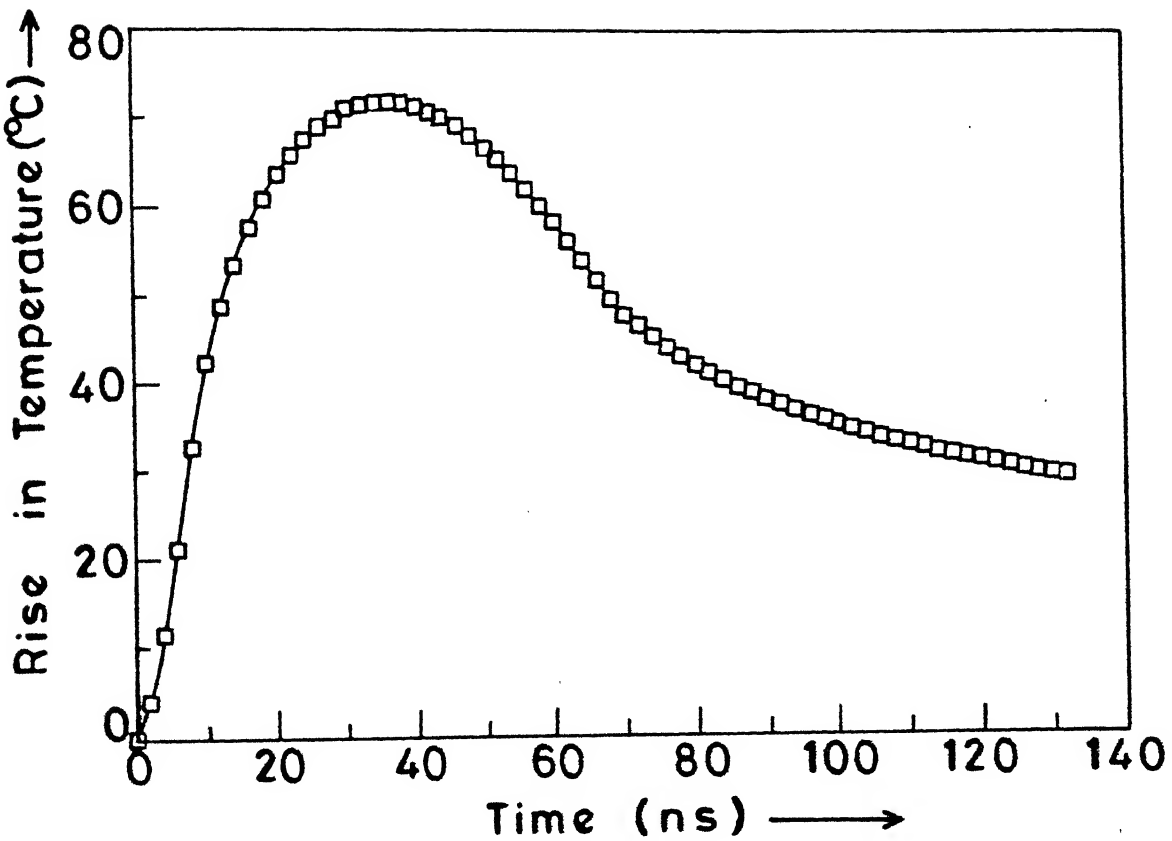

Figure 18 Rise in surface temperature with time

TABLE 1.

Estimated Thermionic current density and photocurrent density for various values of x, the defocussing parameter.

	x = 8 mm	x = 12 mm	x = 17 mm	x = 22 mm
Estimated Intensity at the Surface W/cm^2	$4.74X10^{6}$	$2.84X10^{6}$	$2.00X10^{6}$	$1.42X10^{6}$
Surface Temperature $^{0}_{K}$	420.05	371.93	350.65	335.97
Thermionic current density, j_{th} Amp/cm^2	$4.19X10^{-47}$	$3.70X10^{-54}$	$6.86X10^{-58}$	$9.73X10^{-61}$
Photocurrent density, i Amp/cm^2	$1.00X10^{-9}$	$3.56X10^{-4}$	$1.77X10^{-4}$	$9.00X10^{-5}$

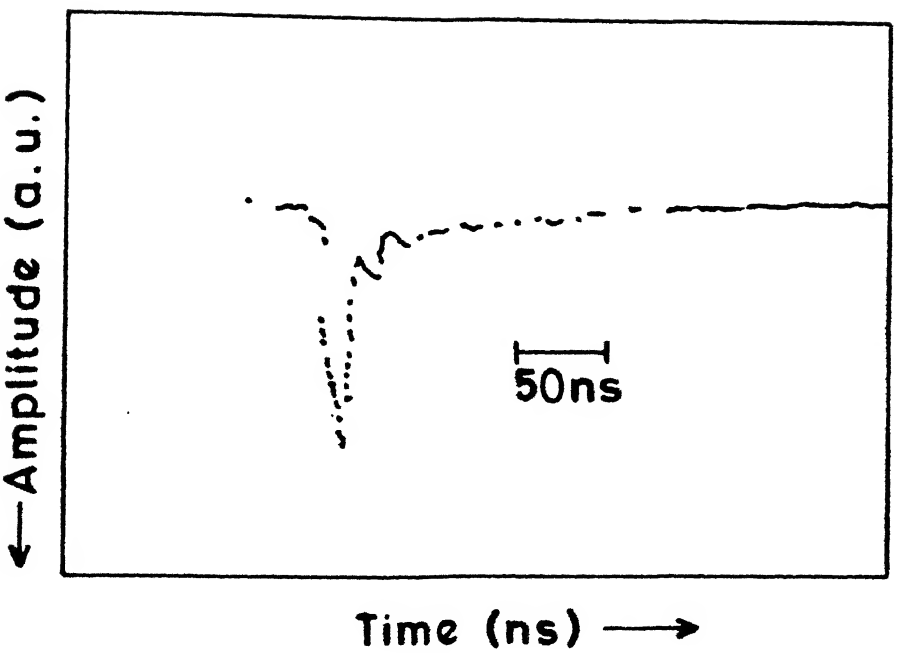

Figure 19 Oscilloscope trace of photoelectric pulse.

in the peak of two pulses (except the built in delay of the recording system viz photomultiplier tube etc), and the photo-electric current pulse is narrow. However, in the case of thermionic emission there should be a delay between the maximum of induced electron pulse and the peak of the laser pulse, and the electron pulse should be broad [6]. Similar results follow from Figure 18. Assuming the laser pulse to be Gaussian, $I = I_o \exp[-t^2/\tau_L^2]$, from the intensity dependence of photo-electric current $i \propto I^n$ it follows that the electron pulse is also Gaussian [92] $i = i_o \exp(-t^2/\tau_E^2)$ with $\tau_E = \tau_L/(n)^{1/2}$. Using this relation between widths of photocurrent pulse τ_E, and of laser pulse τ_L, the exponent n is evaluated, (for the present experimental values τ_E= 19.00 ns and τ_L= 26.4 ns) as $n \approx 2$. To estimate the two photon photoelectric current density, we follow Bloch [93] and Teich et al [94] to calculate the total number of excited electrons, N per second,

$$N = \pi \left[\frac{\Omega\, r_o^2\, m\, C^2\, I_1^2}{2(h\nu)^3\, \nu} \right] \frac{4\pi}{3} \left[\frac{E_F}{2h\nu} \right] k_F \left[1 + \frac{E_\phi}{E_F} - \frac{2h\nu}{E_F} \right]^{3/2} \qquad (7).$$

where $I_1 = I_o(1-R)$ and $k_F = [2\, m\, E_F / \hbar^2]^{1/2}$

For copper, we have E_F = 7.04 eV, E_ϕ = 4.48 eV, the above equation gives $N = 6.47 \times 10^7\, \Omega\, I_1^2$ per sec. therefore $i = 6.47 \times 10^7\, \Omega\, I_1^2 e$ Amp. where volume Ω of the emitting surface

is the area times the depth from which photoelectrons can escape from the metal (we take this depth as 10 Å) [93] and I_o is the intensity in W/mt^2. Values of two photon photoelectric current density for various values of x are evaluated and listed in Table 1. At x = 12 mm it is 3.56×10^{-4} Amp/cm^2. On comparing the values of thermionic current density and photocurrent density for various values of x, we conclude that in our case electron emission due to two photon-photo electric effect dominates over the thermionic effect. The decrease in ionization current of argon gas (Figure 16) may be attributed to the decrease in two photon-photo electric current density with increase in x.

In conclusion investigations of the laser induced breakdown of argon gas near metal surface using a low power excimer laser in the presence of a transverse static electric field are reported. It is observed that threshold laser energy required to breakdown argon gas is reduced in presence of metal surface. Photoelectric emission from metal surface dominates over the thermionic emission and reduces the threshold laser energy for breakdown. Ionization current due to breakdown of argon is observed to be dependent on laser induced photoemission from target surface.

CHAPTER 5

LASER PRODUCED COPPER PLASMA

Introduction

There are several reports on the possibility of observing a high density, high temperature plasma by focusing laser beam on to a solid target [7] or in a gas [5]. Laser produced metal vapor plasma in the presence of a background gas has been used as an active medium for getting laser oscillations [13]. Simultaneously, there have been reports on photoionization/photoexcitation [72,73] of gases by laser produced metal plasma where short wavelength radiation emitted from the metal plasma ionizes/excites the background gas. Recently, there have been reports [95] on studies of plasma produced by UV excimer radiation of moderate intensities. Moderate or low power excimer laser produced plasmas are used for laser material processing [96], and laser microspectral analysis. In the laser microspectral analysis [18,19] a laser radiation is focused on to the target surface to produce plasma and the emitted radiation from the plasma is analyzed for trace elements. Using this method [18] one can easily determine concentration $\leq 0.001\%$. High power excimer laser produced plasmas are of special interest as a source of short wavelength radiation [16]. We have reported laser induced gas breakdown in the presence of TSEF [65] and near metal surface [74] using a

low power excimer laser. Here we report the studies [79] on laser produced copper plasma in the presence of background gas and in vacuum, using XeCl (308 nm) excimer laser.

Experimental Set Up

A schematic of the experimental setup used is shown in Figure 4. The radiation from an excimer laser, XeCl (308 nm) TE-861 M-2 Lumonics Inc. Canada) delivering 3.5 mJ in 25 ns, at 10 pps, was focused on to a copper target enclosed in a glass cell using a quartz lens of focal length 12 cm. The cell was evacuated to a pressure of $\leq 10^{-4}$ torr and then filled in with different gases at desired pressures. Plasma radiation was focused on to the entrance slit of a monochromator (HRS-2 Jobin Yvon, France) so as to have one to one correspondence with the plasma and its image on to the slit of monochromator. The output from the monochromator was detected with a photomultiplier tube (PMT) (1P 28 Hamamatsu, Japan), and recorded on the strip chart recorder in conjunction with a microprocessor controlled scan system (MCSS). The temporal variation of the emitted spectral lines were recorded with 50 ohms termination at PMT output and displayed on the storage oscilloscope (TS 8123 Iwatsu, Japan).

In the following we report the studies on spatial and temporal behavior of the emission spectrum of excimer laser produced copper plasma in vacuum and in the presence of argon

and neon gases. An attempt is made to estimate the temperature and velocity of propagation of plasma emission front.

Results and Discussions

On focusing the laser radiation on to a copper target, a bright green radiation, (with and without background gas) was observed [78] with intensities of laser as low as $\simeq 10^7$ W/cm^2. No radiation from the plasma of background gas was observed when laser radiation was focused on to the copper target and near the target in the gas. Following eqn (3), electron cascade will develope to breakdown argon gas with XeCl laser, only if $I > 2.49 \times 10^{10}$ W/cm^2, which is much greater than the laser intensity used in the present experiment, $\simeq 10^8$ W/cm^2. Moreover, in our case laser power is also not high enough to provide highly ionized copper plasma and hence short wavelength radiation emitted from copper plasma is not available to photoionize the background gas either. Thus we had only copper plasma and no radiation from the background gas.

Figure 20 shows a part of the visible spectrum in copper in vacuum at laser irradiation of 10^8 W/cm^2. Emitted spectral lines were identified [97] and transitions assigned [98] based on existing literature. Figure 20 shows only those transitions which are considered for the present studies.

An extensive study of spontaneously emitted Cu I transitions $4p\ ^2P_{3/2} - 4s^2\ ^2D_{5/2}$ at 510.5 nm, $4d\ ^2D_{5/2} - 4p\ ^2P_{3/2}$ at 521.8 nm

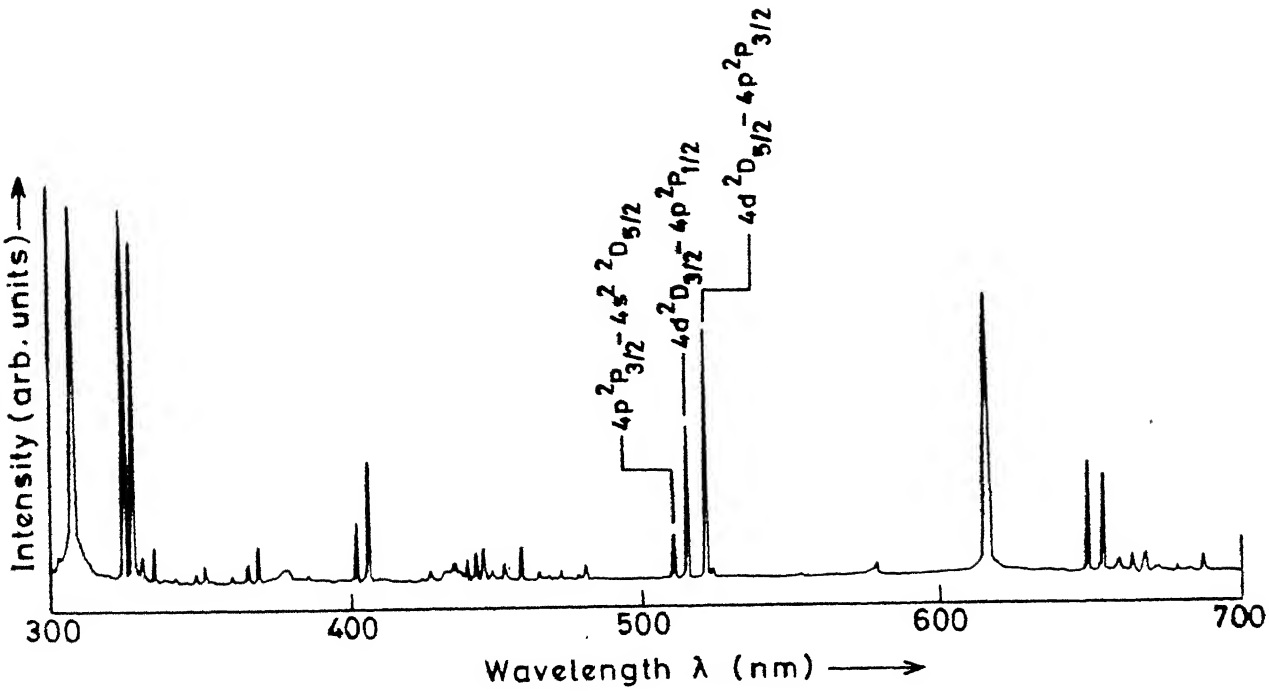

Figure 20 Visible spectrum of copper in vacuum

and 4d $^2D_{3/2}$ - 4p $^2P_{1/2}$ at 515.3 nm was undertaken. We report the spatial variation of intensity of emitted lines with respect to x_p, distance from metal surface and the pressure of the background gas. The variation with x_p was achieved by moving the lens in the direction of the expansion of the plasma. Every point in the figures to follow is an average of five observations. Figure 21 shows the variation of line intensity with x_p in vacuum and in the presence of argon gas at pressure of 8 torr. It is observed that the intensity of emitted spectral lines increases in the presence of background gas. It is also observed that in vacuum the line intensity peaks at the surface and decreases as x_p increases. However, in the presence of argon gas at a pressure of 8 torr the intensity is maximum at x_p=2 mm. The fast initial rise at x_p = 2 mm may be due to rapid cooling of the plasma. Thus the formation of Cu I may be due to recombination of Cu II ions in the afterglow. The recombination rate coefficient of ions of charge Z being given by [99]

$$\alpha = C(Z)T_e^{-9/2} \qquad (8).$$

$$\text{with } C(Z) = 9.2 \times 10^{-39}\ Z^3\ \ln\ (Z^2+1)^{1/2}$$

The rate is thus strongly dependent on electron temperature T_e. The rate of change of electron temperature in the afterglow is sum of three terms [100] viz. the elastic collision, electron heating due to collisional de-excitation of metastable ions and recombination of ions. The rate of loss of electron energy in

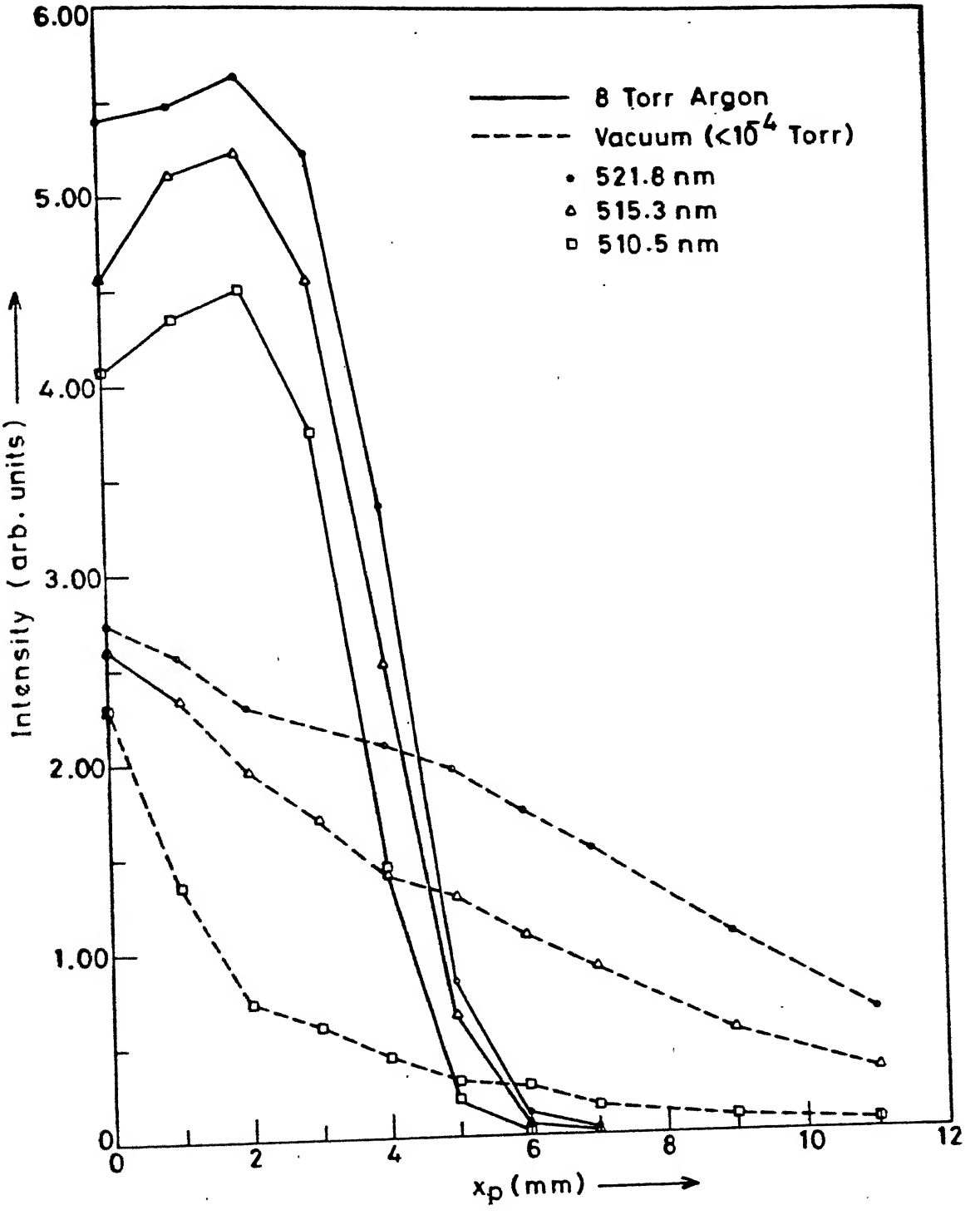

Figure 21 Variation of intensity of Cu I transitions with distance from metal surface, x_p

early stage of afterglow is dominated by the elastic collision term $Q_{\Delta T}$, given by

$$Q_{\Delta T} = \frac{2m_e}{M_B} \sigma_{ea} n_B \left(\frac{8KT_e}{\pi m_e}\right)^{1/2} \qquad (9).$$

where σ_{ea} is the elastic scattering cross section between the electrons and the atoms, n_B is the density of background gas atoms and M_B is the mass of the background gas atom. It follows from eqn (9) that cooling is inversely proportional to M_B and hence lighter gases are efficient for cooling. Next to hydrogen, helium being the lightest inert gas has the possibility of providing more rapid cooling in the afterglow [101]. However, in our studies for the transition $4p\ ^2P_{3/2} - 4s^2\ ^2D_{5/2}$ at 510.5 nm, we have taken neon gas, next to lightest inert gas as the background gas for the reason of its ability to produce stable discharge in Cu-vapor lasers [102]. Figure 22 shows the intensity variation of spontaneously emitted Cu I lasing transition $4p\ ^2P_{3/2} - 4s^2\ ^2D_{5/2}$ at 510.5 nm with pressure of neon gas at x_p = 2 mm. It is observed that the intensity of the line attains a maximum value at a pressure of about 4 torr and then decreases with further increase in pressure. The initial rise shows the rapid cooling of the plasma. The increase in pressure results in reducing the expansion rate and increasing the cooling rate. The enhancement of intensity suggests that at this pressure maximum number of Cu II ions, produced initially,

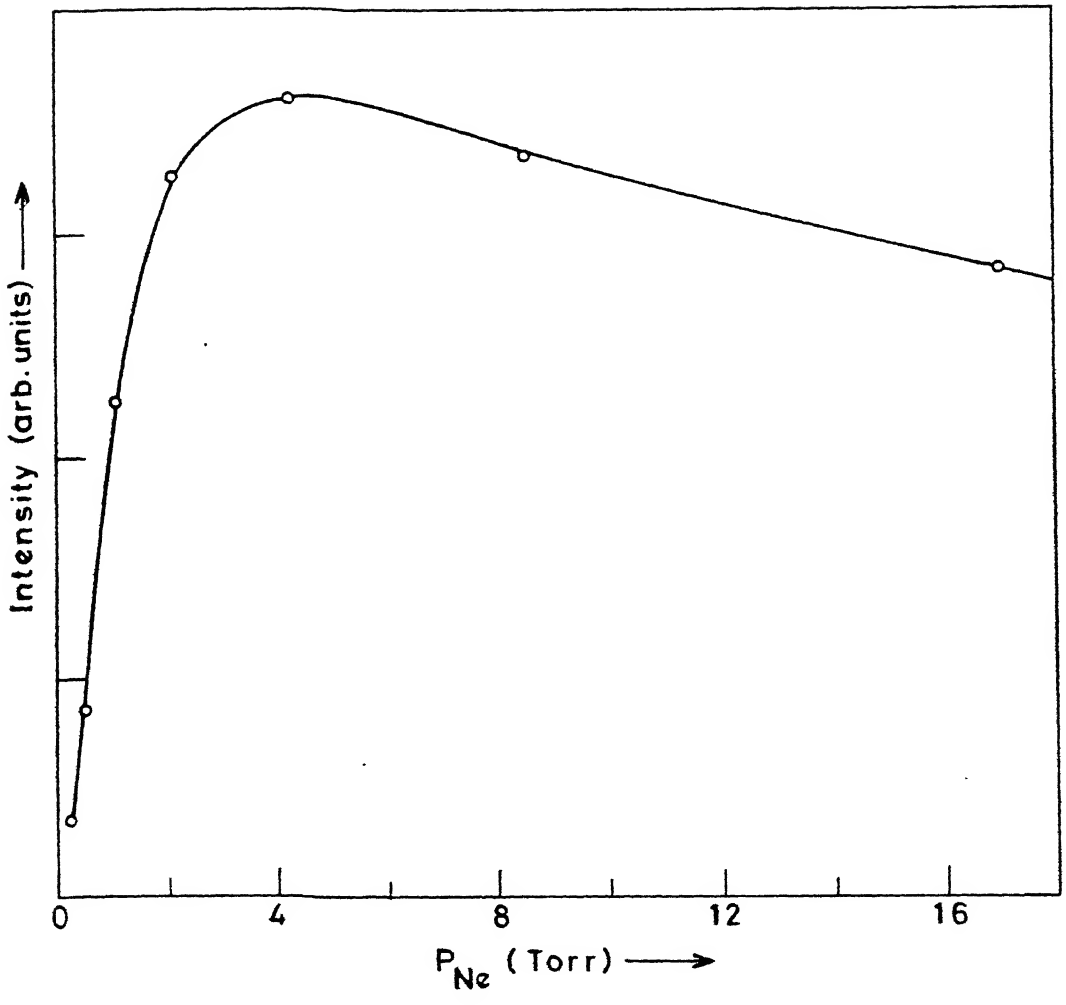

Figure 22 Variation of intensity of transition $4p\ ^2P_{3/2} - 4s^2\ ^2D_{5/2}$ at 510.5 nm with pressure of neon gas.

recombine to give Cu I transition. The decrease of intensity at high pressure is due to very high cooling rate. Figure 21 shows that intensity of Cu I transitions is more in presence of argon gas than that in vacuum. In vacuum, plasma expands freely, electron density decreases faster than the electron temperature. However, in the presence of background gas plasma is confined to a small region, resulting in reduced expansion rate and hence enhanced cooling rate which enhances the intensity of emitting lines.

The plasma temperature was estimated, by assuming that the plasma is in Local Thermodynamic Equilibrium (LTE)and by taking the ratio of intensity of two spectral lines [103] and using the relation

$$KT_e = \frac{E' - E}{\ln (I\lambda g' A_p' / I'\lambda' g A_p)} \qquad (10).$$

where E and E' are the excitation energies of the levels, I's are the intensity; g, A_p and λ are the respective statistical weight, transition probability and wavelength of transition under consideration. The temperature is estimated to lie in the range 0.6 ev $\leq T_e \leq$ 0.8 ev for Cu I in the presence of argon gas at a pressure of 8 torr.

Figure 23 shows the temporal behavior of Cu I transition $4d\ ^2D_{5/2} - 4p\ ^2P_{3/2}$ at 521.8 nm in the presence of argon gas at

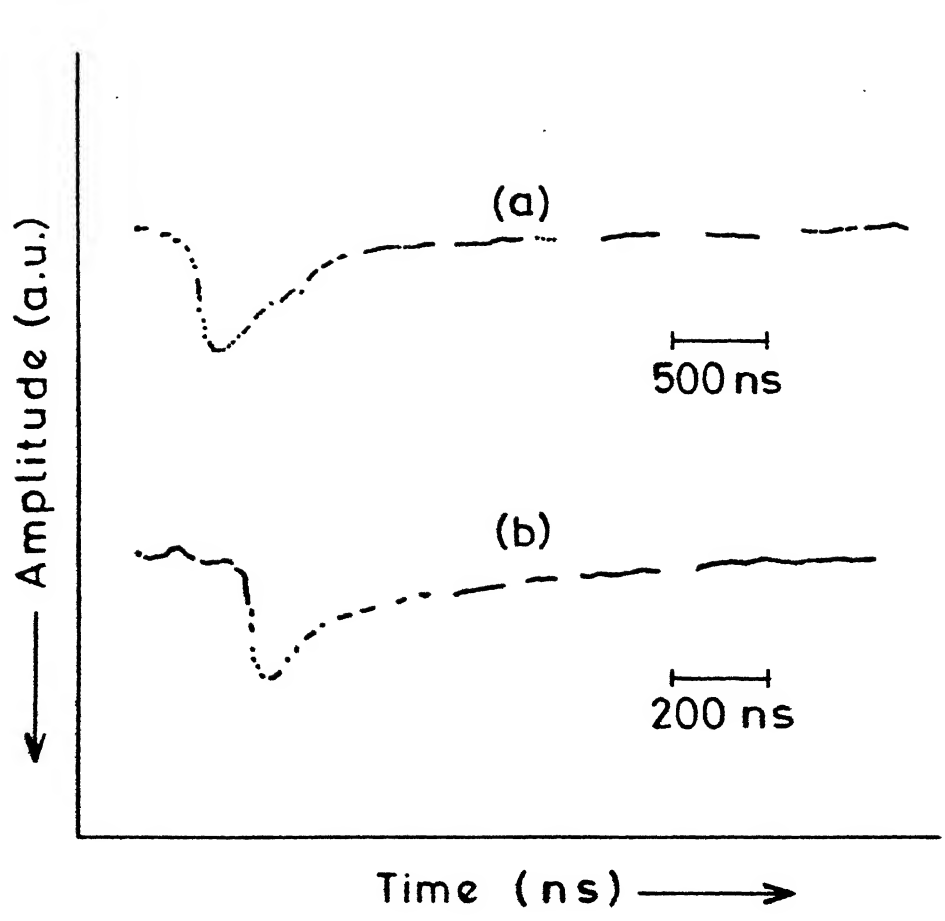

Figure 23 Variation of intensity of transition 4d $^2D_{5/2}$ - 4p $^2P_{3/2}$ at 521.8 nm with time for x_p = 3 mm (a) argon pressure of 8 torr (b) Vacuum

a pressure of 8 torr and in vacuum ($\sim 10^{-4}$ torr) at x_p = 3 mm. To estimate the velocity of plasma emission front as a function of distance x_p, the temporal pulses at different x_p were recorded and the delay in the peak intensity as shown in Figure 24 was measured. It follows from Figure 24 that the velocity of propagation of the plasma emission front at 3 mm away from the target surface is 4.8×10^5 cm/sec in argon gas at a pressure of 8 torr and 1.5×10^6 cm/sec in vacuum. The reduced propagation of the plasma emission front in the presence of argon gas increases the duration of emission as shown in Figure 23a compared to that in vacuum, Figure 23b.

In conclusion we have reported the studies of metal plasma formed in vacuum and in the background gas by focusing the XeCl laser radiation on to the metal surface. It is observed that spontaneously emitted Cu I lasing transition $4p\ ^2P_{3/2} - 4s^2\ ^2D_{5/2}$ at 510.5 nm shows a strong dependence on the pressure of neon gas. We report the possibility of getting copper vapor lasing transition $4p\ ^2P_{3/2} - 4s^2\ ^2D_{5/2}$ at 510.5 nm due to recombination in the presence of neon gas. The velocity of propagation of plasma emission front is found to be less in the case of background gas than that for in vacuum. We observe that intensity of many spectral lines increases in the presence of background gas. The presence of surrounding gas can thus improves the accuracy of laser microspectral analysis.

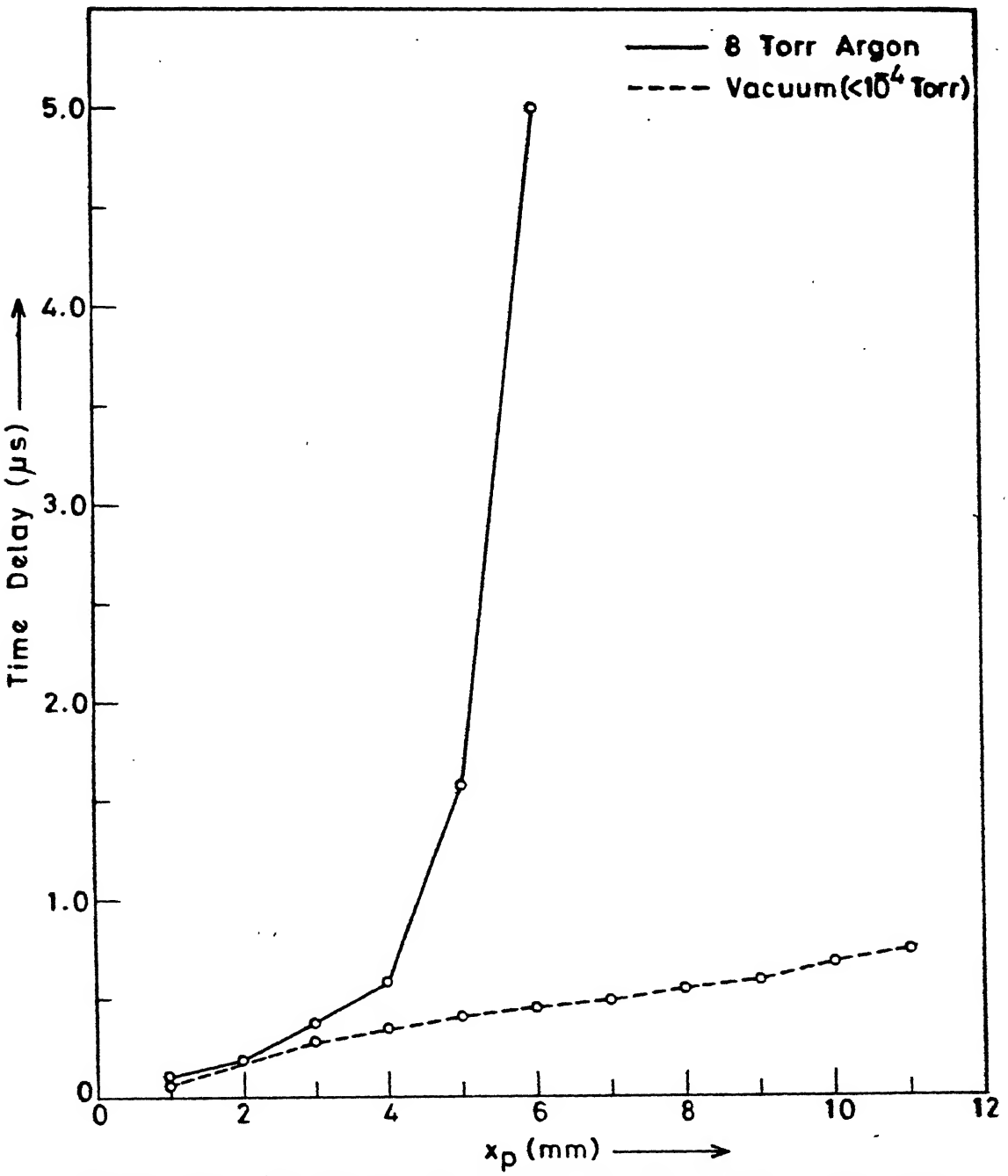

Figure 24 Variation of delay in the peak intensity of the transition 4d $^2D_{5/2}$ - 4p $^2P_{3/2}$ at 521.8 nm with x_p

CHAPTER 6

LASER INDUCED GAS BREAKDOWN : A PLASMA SWITCH

Introduction

There have been reports on the gas breakdown using focused high intensity laser beam alone [5] and in the presence of static electric field [64,65]. Breakdown of gases have been reported at the surface of metallic target [66], with [72] and without [67,74] metal plasma. The effect of metallic target on the laser induced breakdown of argon gas was discussed on the basis of photoelectron emission [74] from the target surface. We have discussed in earlier chapters the studies on laser induced breakdown of gases in the presence of TSEF and near metal surface. Some studies on laser produced metal plasma are also discussed. Here we report [104] for the first time; the effect of metal plasma formed at the surface of a biased target on the laser induced argon gas breakdown and explore the possibility of a plasma switch. We observed that the effect of metal plasma is identical to the function of grid between the anode and cathode in triode.

Experimental Setup

Experimental arrangement is similar to that of one described in chapter 2. It consists of a specially designed glass cell having two parallel brass plates (20x25 mm^2)

separated by 6.5 mm and a copper target at a distance of 15 mm from the edge of the parallel plates as shown in Figure 2. The cell was evacuated to a pressure of $<10^{-4}$ torr and then filled in with argon gas at a pressure of 8 torr. A bright green metal plasma is observed by focusing (f=12cm) an XeCl (308 nm) excimer laser delivering 3.5 mJ in 25 ns at 10 pps on to the copper target. As described in Chapter 4 the best focusing of the laser radiation on to the copper target is defined as x = 0. The irradiation on to the target and hence the extent, size of plasma is reduced by moving the lens away from the copper target on the same optic axis. Copper target is biased positive or negative w.r.t. brass plate using an EG & G power supply. Breakdown of argon gas due to laser radiation was observed visually by the appearance of glow discharge modulating at 10 pps. The effect of metal plasma on laser induced breakdown of argon gas in various configuration of biased target and plate is described below.

Results and Discussions

Static glow discharge of argon gas was observed when a static voltage of 0.58 KV was applied between the target and plate. However, when laser radiation is focused or defocused depending on the polarity of the target as shown in Figures 25, pulsed glow discharge modulating at 10 pps was observed with

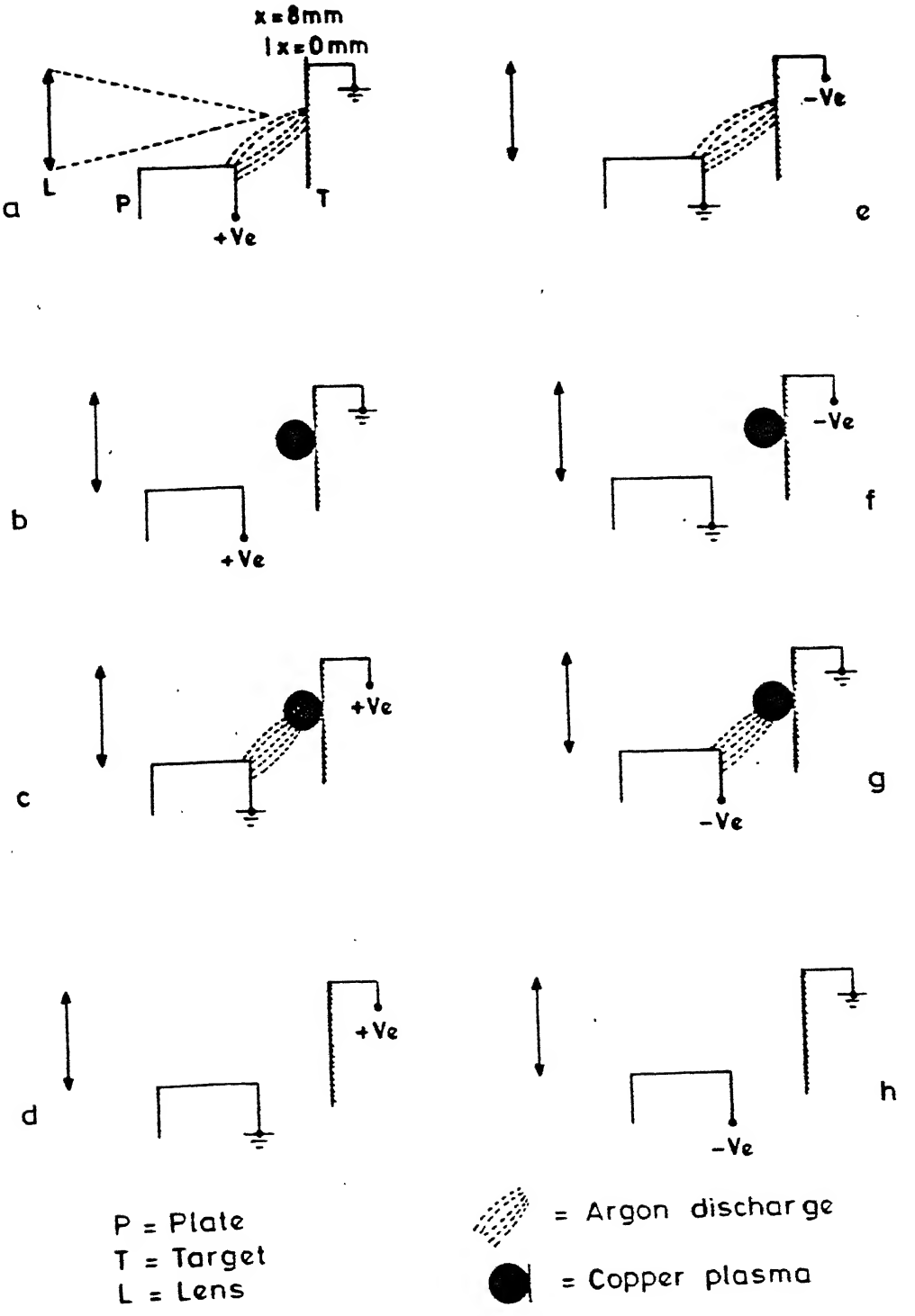

Figure 25 Schematic sketches of visual observation of laser induced gas breakdown in various configurations of biased target with focussing geometry

static voltage of 0.32 KV. For the sake of clarity only Plate (P) Target (T) and Lens (L) are shown in the Figure 25.

Case 1. Static voltage is applied across plate (+ve) and target (ground) as shown in Figures 25a and 25b. We observe pulsed discharge in the region between plate and target only in the configuration of Figure 25a when laser is defocused by 8 mm. At this position copper plasma was not visible and only source of initiating breakdown is the photoelectron [74] emitted from the copper surface. The emitted electrons gain enough energy in the static field and ionize the argon gas by inelastic collisions. However, when laser radiation is focused on to the copper target a bright green plasma appears and argon discharge disappears as shown in Figure 25b. In this configuration the electrons will be attracted towards the +ve plate and a sheath is formed at a distance of λ_D; debye length [105],

$$\lambda_D(\text{meter}) = \left[\frac{\varepsilon_o K T_e}{n_e e^2}\right]^{1/2} \qquad (11).$$

Even if we assume minimum electron density, $n_e \simeq 10^{15}$ mt^{-3} and temperature [78], $T_e \simeq 0.8$ ev, debye length is 210 μm. Thus positive potential is screened off beyond 210 μm and argon discharge disappears.

Case 2: Static voltage is applied across target (+ve) and plate (ground) as shown in Figures 25c and 25d. Unlike Case 1, here we

observe argon discharge only in the presence of copper plasma as shown in Figure 25c. The effect of plasma is essentially to shift the position of positive potential by a distance equal to the size of plasma, $\simeq$ 7 mm. This results in decrease in the virtual distance between target and plate and hence increase in electric field resulting in breakdown of argon gas. However, if the laser radiation is defocused by 8 mm as shown in Figure 25d, the argon discharge disappears due to decrease in electric field. The possibility of photoelectrons is also ruled out as target is positive.

Case 3: Static voltage is applied across plate (ground) and target (-ve) as shown in Figures 25e and 25f. Agron discharge appears only when laser is defocused by 8 mm as shown in Figure 25e. Situation is identical to Figure 25a, target being at lower potential than the plate, photoelectrons emitted from target surface are accelerated towards the plate, gain energy and ionize the argon gas by inelastic collision. However, with focused laser radiation as shown in Figure 25f, we have situation similar to Figure 25b where sheath formation prevents the argon discharge.

Case 4: Static voltage is applied across target (ground) and plate (-ve) as shown in Figures 25g and 25h. The situation is opposite to Case 3 and similar to Case 2, target being at higher

potential, we observe argon discharge with focused laser radiation which disappears on defocussing the radiation.

In conclusion, we observe that ionization of argon gas can be switched ON or OFF either keeping laser focusing conditions fixed and by changing the polarity (combinations shown in Figures 25a and 25h; 25b and 25g; 25c and 25f; 25d and 25e) OR keeping the polarity fixed and by changing the laser radiation from focused to defocused state (combinations shown in Figures 25a and 25b; 25c and 25d; 25e and 25f; 25g and 25h).

CHAPTER 7

CONCLUSIONS

We reported studies on the excimer laser induced breakdown of rare gases in the presence of (a) static electric field and (b) metal surface in a specially designed discharge cell. Some studies on laser produced plasma are also presented. Utilizing the effect of metal plasma on laser induced breakdown of argon gas in various configurations of biased target we propose the possibility of a plasma switch.

Breakdown of neon, argon and xenon gases in the range of pressure 0.2 - 24.0 torr is studied by focusing a low power excimer laser in the presence of static electric field transverse to the laser focus. Our results are similar to that observed by other investigators using high power lasers alone. We propose ionization to be a two step process, initial excitation being through collision of atoms with electrons due to static electric field followed by photoionization in the presence of laser. We report for the first time that k_o, the number of photons actually involved to ionize the gas in the experiment, decreases with the increase of static electric field. These studies are important for designing fast switching devices and joule meter to measure the energy of high power lasers.

Laser induced breakdown of argon gas near metal surface is studied by using low power excimer laser in the presence of TSEF. We report for the first time that photoelectric emission from metal surface dominates over the thermionic emission and reduces the threshold laser energy required to breakdown argon gas. Ionization current is observed to be dependent on laser induced photoelectric emission from target surface. These studies are helpful for achieving electron pulses of short duration and to understand the mechanism of laser induced gas breakdown with low power lasers.

Spatial and temporal behavior of the emission spectrum of excimer laser produced copper plasma in vacuum and in the presence of background gases are studied. It is observed that spontaneous emission from Cu I lasing transition $4p\ ^2P_{3/2} - 4s^2\ ^2D_{5/2}$ at 510.5 nm shows a strong dependence on the pressure of neon gas. We report the possibility of getting copper vapor lasing transition $4p\ ^2P_{3/2} - 4s^2\ ^2D_{5/2}$ at 510.5 nm as a result of recombination in presence of neon gas. The plasma temperature was estimated by assuming the plasma to be in Local Thermodynamic Equilibrium (LTE) and by taking the ratio of intensity of two spectral lines. The temperature is estimated to lie in the range 0.6 ev $\leq T_e \leq$ 0.8 ev for Cu I in the presence of argon gas at a pressure of 8 torr. The velocity of propagation of the plasma emission front at 3 mm away from the target

surface is found to be less in the presence of background gas than that for in vacuum. It is also observed that intensity of many emitted spectral lines increases in the presence of background gas. The presence of surrounding gas can thus improves the accuracy of laser microspectral analysis.

The effect of metal plasma formed on the surface of a biased target on laser induced breakdown of argon gas is studied in various configurations of biased target. It is observed that the effect of metal plasma in our studies is identical to the function of a grid between anode and cathode in a triode. We report for the first time that ionization of argon gas can be switched ON or OFF either keeping laser focusing conditions fixed and by changing the polarity OR keeping the polarity fixed and by changing the laser irradiation.

Future work

In order to gain more understanding on the mechanism of laser induced gas breakdown in the presence of static electric field, more work on the dependence of breakdown threshold on pressure, focal spot size and laser parameters: pulse width and wavelength is required. To study the rate of ionization growth w.r.t. laser pulse, systematic temporal studies should be undertaken. In order to gain more understanding on the mechanism of laser induced gas breakdown near metal surface, more studies

using targets of different work function which can provide single, double or triple photon photo-electric effect have to be undertaken. Studies will help in achieving electron pulses of short duration. The similar experiment can also be performed by keeping the target fixed and changing the wavelength of laser radiation.

A systematic study should be undertaken to measure the plasma parameters; electron density and temperature, for various input parameters *eg* laser power and pressure of background gas to optimize lasing conditions in copper vapor plasma. It may be possible to observe metal vapor lasers in high melting point metals with low power lasers where metal vapors produced by irradiating the metal targets are excited/ionized by pulsed discharge.

To have commercially viable plasma switches, technological aspects have to be considered.

REFERENCES

[1] P.D. Maker, R.W Terhune, and C.M. Savage, Proceedings of the 3rd International Conference on Quantum Electronics, edited by P. Grivet, and N. Blombergen (Columbia, New York, 1963), pp 1559-1565.

[2] R.G. Mayerand and A.F. Haught, Phys. Rev. Lett. **11**, 401 (1963).

[3] P. Agostini, G. Barjot, G. Mainfray, C. Manus, and J. Thebault, IEEE, J. Quant. Electron QE-6, 782 (1970).

[4] C. Grey Morgan, Rep. Prog. Phys. **38**, 621 (1975).

[5] P. Agostini and G. Petite, Contemp. Phys. **29**, 57 (1988).

[6] J.F. Ready, in Effects of high power laser radiation, (Academic Press, New York, 1971).

[7] E.T. Kennedy, Contemp. Phys. **25**, 31 (1984).

[8] A.H. Guenther and J.K. Bettis, J. Phys. D: Appl. Phys. **11**, 1577 (1978).

[9] J. Nuckolls, J. Emmett, and L. Wood, Phys. Today **26**, 46 (1973).

[10] N.S. Kopeika, R. Gellman, and A.P. Kushelevsky, Appl. Opt. **16**, 2470 (1977).

[11] P. Laporte, N. Damany, and H. Damany, Opt. Lett. **12**, 987 (1987).

[12] W.T. Silfvast, L.H. Szeto, and O.R. Wood II, J. Appl. Phys. **50**, 7921 (1979).

[13] W.T. Silfvast, L.H. Szeto, and O.R. Wood II, Opt. Lett. **4**, 271 (1979).

[14] M.H. Key, J. Mod. Opt. **35**, 575 (1988).

[15] C. Chenais-Popovics, R. Corbett, C.J. Hooker, M.H. Key, G.P. Kiehn, C.L.S. Lewis, G.J. Pert, C. Regan, S.J. Rose, S. Sadaat, R. Smith, T. Tomie, and O. Willi, Phys. Rev. Lett. **59**, 2161 (1987).

[16] Y. Matsumoto, M.J. Shaw, F.O' Neill,J.P. Partanen, M.H. Key, R. Eason, I.N. Ross, E.M. Hadgson, and Y. Sakagami, Appl. Phys. Lett. **46**, 28 (1985).

[17] W.T. Silfvast and O.R. Wood II, J. Opt. Soc. Am. **B4**, 609 (1987).

[18] K. Kagawa and S. Yokoi, Spectrochimica Acta **B 37**, 789 (1982)

[19] R.S. Adrain and J. Watson, J. Phys. D: Appl. Phys. **17**, 1915 (1984).

[20] A Gold and H.B. Bebb, Phys. Rev. Lett. **14**, 60 (1965).

[21] H.B. Bebb and A. Gold, Phys. Rev. **143**, 1 (1966).

[22] V.M. Morton, Proc. Phys. Soc. **92**, 301 (1967).

[23] G.S. Voronov, Sov. Phys. JETP **24**, 1009 (1967).

[24] F.T. Chan and C.L. Tang, Phys. Rev. **185**, 42 (1969).

[25] Y. Gontier and M. Trahin, Phys. Rev. **172**, 83 (1968).

[26] D.C. Smith, Appl. Phys. Lett. **19**, 405 (1971).

[27] G.J. Pert, IEEE, J. Quant. Electron. **QE-8**, 623 (1972).

[28] Y. Gontier and M. Trahin, Phys. Rev. A **7**, 1899 (1973).

[29] L.V. Keldysh, Sov. Phys. JETP **20**, 1307 (1965).

[30] L. Mandel and E. Wolf, Rev. Mod. Phys. **37**, 231 (1965).

[31] G.S. Agarwal, Phys. Rev. A **1**, 1445 (1970).

[32] G.S. Voronov, G.A. Delone, and N.B. Delone, JETP Lett. **3**, 313 (1966).

[33] P.N. Krasyuk, P.P. Pashinin,and A.M. Prokhorov, Sov. Phys. JETP **31**, 860 (1970).

[34] P.N. Krasyuk, P.P. Pashinin,and A.M. Prokhorov, JETP Lett. **9**, 354 (1969).

[35] G. Baravian, R. Benattar, and G. Sultan, Appl. Phys. Lett. 25, 291 1974.

[36] G. Baravian, J. Godart, and G. Sultan, Appl. Phys. Lett. **36**, 415 1980.

[37] S.L. Chin, N.R. Isenor, and M. Young, Phys. Rev. **188**, 7 (1969).

[38] S.L. Chin and N.R. Isenor, Can. J. Phys. **48**, 1445 (1970).

[39] T. Okuda, K. Kishi, and K. Sawada, Appl. Phys. Lett. **15**, 181 (1969).

[40] K. Kishi, K. Sawada, and T. Okuda, J. Phys. Soc. Japan **29**, 1053 (1970).

[41] K. Kishi and T. Okuda, J. Phys. Soc. Japan **31**, 1289 (1971).

[42] A.J. Alcock and M.C. Richardson, Phys. Rev. Lett. **21**, 667 (1968).

[43] R.J. Dewhurst, G.J. Pert, and S.A. Ramsden, in Proc. 10^{th} Int. Conf. Phenomena Ionized Gases, (Oxford, 1971) pp 220.

[44] Yu. P. Raizer, Sov. Phy. JETP **21**, 1009 (1965).

[45] H. Buscher, R. Thomlinsen, and E. Damon, Phys. Rev. Lett. **15**, 847 (1965).

[46] A. Alcock, K. Kato, and M. Richardson, Opt. Commun. **6**, 342 (1972).

[47] R.J. Dewhurst, G.J. Pert, and S.A. Ramsden, J. Phys. B: Atom. Molec. Phys. **7**, 2281 (1974).

[48] C.L.M. Ireland and C. Grey Morgan, J. Phys. D: Appl. Phys. **7**, L87 (1974).

[49] F. Morgan, L.R. Evans, and C. Grey Morgan, J.Phys. D: Appl. Phys. **4**, 225 (1971).

[50] V.E. Mitsuk, V.I. Savoskin, and V.A. Chernikov, JETP Lett. **4**, 88 (1966).

[51] V.E. Mitsuk and V.A. Chernikov, JETP Lett. **6**, 124 (1967).

[52] G. Weyl, D. Rosen, J. Wilson, and W. Seka, Phys. Rev. **A26**, 1164 (1982).

[53] G. Weyl and D. Rosen, Phys. Rev. **A31**, 2300 (1985).

[54] I. Krasyuk and P. Pashinin, JETP Lett. **15**, 33 (1972).

[55] D.I. Rosen and G. Weyl, J. Phys. D: Appl. Phys. **20**, 1264 (1987).

[56] N. Kroll and K.M. Watson, Phys. Rev. **A5**, 1883 (1972).

[57] Y. Gamal and M. Harith, J. Phys. D: Appl. Phys. **14**, 2209 (1981).

[58] David C. Smith, J. Appl. Phys. **41**, 4501 (1970).

[59] A.M. Robinson, Appl. Phys. Lett. **22**, 33 (1973).

[60] R.T. Brown and D.C. Smith, Appl. Phys. Lett. **22**, 245 (1973).

[61] N.S. Kopeika, G. Eytan, and A.P. Kushelevsky, J. Appl. Phys. **50**, 11 (1974).

[62] J. Tulip and H. Seguin, Appl. Phys. Lett. **23**, 135 (1973).

[63] A.M. Howatson, in An introduction to Gas Discharges (Pergaman, London, 1965).

[64] N. Yackerson and N.S. Kopeika, IEEE, J. Quant. Electron. **QE-21**, 1728 (1985); **QE-21**, 1964 (1985).

[65] V. Kumar and R.K. Thareja, J. Appl. Phys. **64**, 5269 (1988).

[66] A.N. Pirri, R. Schlier, and D. Northam, Appl. Phys. Lett. **21**, 79 (1972).

[67] A.V. Bondarenko, V.S. Golubev, E.V. Dan'shchikov, F.V. Lebedev, A.F. Nastoyashchii, and A.V. Ryazanov, Sov. Phys. Dokl. **25**, 616 (1980).

[68] A.A. Vedenov, G.G. Gladush, and A.N. Yavokhin, Sov. J. Quant. Electron. **11**, 896 (1981) and references therein.

[69] E.V. Dan'shchikov, V.A. Dymshakov, F.Y. Lebedev, and A.V. Ryazanov, Sov. J. Quant. Electron. **12**, 62 (1982); ibid **12**, 67 (1982).

[70] A.I. Barchukov, F.V. Bunkin, V.I. Konov, and A.A. Lyubin, Sov.Phys. JETP **39**, 469 (1974).

[71] J. Bruneteau and E. Fabre, Phys. Lett. **39A**, 411 (1972).

[72] M.G. Drouet, Appl. Phys. Lett. **31**, 647 (1977).

[73] J.M. Green, W.T. Silfvast, and O.R. Wood II, J. Appl. Phys. **48**, 2753 (1977).

[74] V. Kumar and R.K. Thareja (Submitted).

[75] A. Wasserman, Appl. Phys. Lett. **10**, 132 (1967).

[76] Y.R. Shen, in the Principles of Non-linear Optics (John Wiley, New York, 1984).

[77] Gy Farkas, Z. Gy Horvath, and I. Kertesz, Phys. Lett. **39A**, 231 (1972).

[78] V. Kumar and R. K. Thareja , Bull. Am. Phys. Soc. **33**, 1653 (1988).

[79] V. Kumar and R.K. Thareja (Submitted).

[80] Excimer Lasers, edited by Ch. K. Rhodes (Springer-Verlag, Berlin, 1979).

[81] V. Kumar and R.K. Thareja (Submitted).

[82] Kenjo Takashi, in Stepping Motors and their Microprocessor Control (Clarendon Press, Oxford, 1984).

[83] Operational Manual of Microfriend-I (DMS Bombay, India, 1986).

[84] A.P. Malvino, Digital Computer Electronics; An Introduction to microcomputers (Tata McGraw Hill 2nd edition, New Delhi, India, 1986).

[85] W.E. William, M.J. Soileau, and E.W. Van Stryland, Appl. Phys. Lett. **43**, 352 (1983).

[86] D.C. Smith and M.C. Fowler, Appl. Phys. Lett. **22**, 500 (1973).

[87] N.S. Kopeika and A.P. Kushelevsky, Appl. Opt. **17**, 3933 (1978).

[88] N.S. Kopeika, T. Karcher, and C.S. Ih, Appl. Opt. **18**, 3513 (1979).

[89] F. Llewellyn-Jones, in Ionization and Breakdown in Gases, (Chapman and Hall Ltd, London 1966).

[90] L.P.Smith, pp 8-76 and R.J. Maurer, pp 8-67, Handbook of Physics (eds E.U.Condan and H.Odishaw 2nd ed. Mc-Graw Hill, New York).

[91] Jui-teng Lin and T.F. George, J. Appl. Phys. **54**, 382 (1983).

[92] E.M. Logothetis and P.L. Hartman, Phys. Rev. **187**, 460 (1969).

[93] Peter Bloch, J. Appl. Phys. **35**, 2052 (1964).

[94] M.C. Teich and G.J. Wolga, Phys.Rev. **171**, 809 (1968).

[95] E.V. Evstratov, M.F. Kanevskii, A.M. Kovalevich, and Yu. Yu. Stepanov, Sov. J. Quantum Electron **18**, 354 (1988).

[96] A.J. Pedraza, J. of Metals, pp 14 (Feb. 1987).

[97] Joseph Reader, C.H. Corliss, W.L. Wiese, and G.A. Martin, in wavelengths and Transition Probabilities for Atoms and Atomic ions, Nat. Stand. Ref. Data Ser., Nat. Bur. Stand. (USA), (Dec. 1980).

[98] I. Smilanski and L.A. Levin, Opt. Lett. **5**, 93 (1980).

[99] A.V. Gurevich and L.P. Pitaevskii, Sov. Phys. JETP **19**, 870 (1964)

[100] V.V. Zhukov, V.S. Kucherov, E.L. Latush, and M.F. Sem, Sov. J. Quant. Electron. **7**, 708 (1977).

[101] A. Khare, Indian Institute of Technology, Kanpur, India, Ph.D. Thesis, (1987).

[102] K. Kirata and H. Ninomiya, J. Appl. Phys. **64**, 6865 (1988).

[103] A. Khare, V. Kumar, and R.K. Thareja, Z. Phys. D., At. Mol. Clusters **6**, 67 (1987).

[104] V. Kumar and R.K. Thareja (Submitted).

[105] R.A. Cairns, Plasma Physics (Blackie and Son Limited Bishopbriggs, Glasgow G64 2NZ, London, 1985).